

POLITECNICO DI MILANO

School of Industrial and Information Engineering
Master of Science in Telecommunications Engineering
Electronic, Information and Bioengineering Department



Cell Discovery with Directive Antennas in mm-wave 5G Networks

Supervisor: prof. Antonio Capone
Assistant supervisors: prof. Ilario Filippini
dr. Vincenzo Sciancalepore

Denny Tremolada ID 816925

ACADEMIC YEAR 2015/2016

ABSTRACT

The growth of Internet traffic and the increasing relevance of network connections are driving network operators and researchers towards a new standard in mobile communications known as 5G. One of its features is related to the transition from the frequencies in UHF band to the exploitation of the so-called millimeter waves (mm-waves), between 30 and 300 GHz, with a particular attention to the 60 GHz bandwidth, which can offer significant performances in terms of capacity.

The use of these particular frequencies causes a radical change in the transmission mechanisms, limiting their use to microcells with limited coverage. This implies the inability for a network based only on mm-waves to provide a reliable service and the need to maintain a legacy network composed of macrocells and based on lower frequencies. The MiWEBA project therefore proposes a functional split between C-plane and U-plane, respectively dedicated to the transmission of signaling messages by exploiting the macrocells and to high-capacity user transmissions using microcells.

One of the main drawbacks of the use of mm-waves is related to the impossibility to use omnidirectional antennas during cell discovery and the consequent need to exploit beamforming techniques to compensate for the lower coverage. In order to use proper antenna configurations, a localization mechanism allows the BS to obtain information about the positions of the MSs. The entire process can, however, be delayed by the use of unsuitable configurations, due to the inaccuracy of the localization service and the possible presence of obstacles in the propagation environment. The use of algorithms able to define an effective sequence of antenna configurations is thus at the basis of a satisfactory result in terms of time employed during the cell discovery, in addition to the possibility to apply the concept of learning memory and exploit information based on previous transmissions in order to further shorten the duration of the process.

In this thesis work we analyze the behavior of three algorithms in propagation environments characterized by different levels of MS location information accuracy and the possible presence of physical obstacles and the impact of learning memory on the cell discovery process.

SOMMARIO

L'aumento del traffico Internet e l'importanza sempre maggiore delle connessioni di rete stanno spingendo operatori e ricercatori verso la definizione di un nuovo standard nelle comunicazioni mobili noto come 5G. Una delle sue caratteristiche è legata al passaggio dalle frequenze nella banda UHF all'utilizzo delle cosiddette onde millimetriche (mm-waves), comprese tra 30 e 300 GHz, con una particolare attenzione alla banda a 60 GHz, in grado di offrire prestazioni notevoli in termini di capacità.

L'utilizzo di queste particolari frequenze comporta un cambiamento radicale nelle modalità di trasmissione, che ne limita l'uso a microcelle con copertura limitata. Ciò implica l'impossibilità da parte di una rete basata solo su mm-waves di fornire un servizio affidabile e la necessità di mantenere una rete legacy composta da macrocelle e basata su frequenze minori. Il progetto MiWEBA propone dunque una separazione funzionale tra C-plane e U-plane, dedicati rispettivamente alla trasmissione di messaggi di signaling sfruttando le macrocelle e a trasmissioni ad alta capacità agli utenti utilizzando microcelle.

Uno dei principali svantaggi dell'utilizzo delle mm-waves è legato all'impossibilità di usare antenne omnidirezionali durante la cell discovery, e alla conseguente necessità di usare tecniche di beamforming per compensare la minor copertura. Al fine di utilizzare configurazioni di antenna appropriate, un meccanismo di localizzazione permette alla BS di ottenere informazioni sulle posizioni delle MS. L'intero processo può tuttavia essere ritardato dall'utilizzo di configurazioni non adatte, dovuto all'inaccuratezza del servizio di localizzazione e alla possibile presenza di ostacoli nell'ambiente di propagazione. L'utilizzo di algoritmi in grado di definire un'efficace sequenza di configurazioni di antenna è dunque alla base di un risultato soddisfacente in termini di tempo impiegato durante il processo, oltre alla possibilità di applicare il concetto di learning memory e sfruttare le informazioni basate sulle precedenti trasmissioni al fine di ridurre ulteriormente la durata.

In questo lavoro di tesi si analizzano il comportamento di tre algoritmi in ambienti di propagazione caratterizzati da diversi livelli di accuratezza dell'informazione di localizzazione delle MS e dall'eventuale presenza di ostacoli fisici e l'impatto della learning memory nel processo di cell discovery.

TABLE OF CONTENTS

Abstract	i
Sommario	iii
	Page
List of Figures	1
List of Tables	3
1 Introduction	5
2 Introduction to 5G standard	7
2.1 5G overview	7
2.2 5G main requirements	9
2.3 5G application scenarios	13
2.4 5G spectrum opportunities	14
3 Mm-wave access networks	17
3.1 HetNet	17
3.2 Mm-waves main features	19
3.3 Directional transmissions	24
3.4 Advanced network architectures	25
3.4.1 Control and user plane separation	25
3.4.2 C-RAN solutions	26
3.4.3 Green networking solutions	29
3.5 Initial cell discovery	31
4 Algorithms and learning memory procedure	33
4.1 Directional cell discovery	33
4.2 Random discovery algorithm	35
4.3 DGS algorithm	35
4.4 EDP algorithm	36

4.5	Learning memory mechanism	37
4.6	Getting location information	38
5	Numerical results	41
5.1	Propagation model and playground	41
5.2	Obstacle-free scenario	45
5.3	Perfect context information scenario	52
5.4	Realistic scenario	59
5.5	Realistic scenario with MS in the corner	68
6	Conclusions and future developments	73
6.1	Conclusions	73
6.2	Future developments	74
A	Appendix A	77
B	Appendix B	79
C	Appendix C	81
	Bibliography	85

LIST OF FIGURES

2.1	Differences between 4G and 5G technical objectives	9
2.2	Comparison between rates in mobile communication generations	9
2.3	Latency times comparison	10
2.4	HetNet	12
2.5	Modular Antenna Array architecture	13
2.6	Main frequency bands for wireless communications between 2 and 90 GHz	15
2.7	Spectra available around 60 GHz	15
3.1	Signal attenuation at sea level and 20 °C versus log frequency	20
3.2	Rainfall attenuation vs frequency	21
3.3	Proposed architecture for 5G cellular networks	26
3.4	C-RAN architecture model	27
3.5	C-RAN centralized model	28
3.6	Fully centralized and partial centralized architectures	28
3.7	Components of the power consumption of China Mobile	29
3.8	Mobile Network Load in Daytime	30
3.9	Deafness problem	31
3.10	Omnidirectional vs directional antennas coverage	32
4.1	Discovery Greedy Search	36
4.2	Enhanced Discovery Procedure	37
4.3	WiFi fingerprinting-based localization service	39
5.1	Obstacles and MSs location	43
5.2	Comparison between DGS and EDP in a memoryless scenario	45
5.3	Comparison between standard deviation values of the number of switches with DGS and EDP in a memoryless scenario	47
5.4	Average number of switches for a BS-MS connection in an obstacle-free propagation scenario	48
5.5	Comparison between the average number of switches using DGS and EDP without exploiting memory	52

5.6	Reachability prevented by reflection mechanisms	53
5.7	Average number of switches when learning memory is applied	55
5.8	Configuration affected by memory range	56
5.9	Comparison between algorithms in a memoryless 9-obstacle scenario with location errors	59
5.10	Comparison between DGS and EDP in a memoryless obstacle-free and in a memoryless 9-obstacle scenario with location errors	60
5.11	Variation of the number of switches when different accuracy values are applied	63
5.12	Playground representation	66
5.13	New playground representation	68

LIST OF TABLES

2.1	Mobile subscription essentials	8
2.2	Traffic essentials	8
5.1	Saved switches for each memory access with DGS algorithm	49
5.2	Saved switches for each memory access with EDP algorithm	50
5.3	Percentage decrease by learning memory application using DGS algorithm	50
5.4	Percentage decrease by learning memory application using EDP algorithm	51
5.5	Saved switches for each successful memory access with DGS algorithm	57
5.6	Saved switches for each successful memory access with EDP algorithm	57
5.7	Average percentage decrease with DGS algorithm	58
5.8	Average percentage decrease with EDP algorithm	58
5.9	Percentage decrease using DGS algorithm	64
5.10	Percentage decrease using EDP algorithm	64
5.11	Percentage decrease using random algorithm	64
5.12	Average percentage of successful accesses using DGS algorithm	65
5.13	Average percentage of successful accesses using EDP algorithm	65
5.14	Average percentage of successful accesses using random algorithm	66
5.15	Memory content of a generic simulation	67
5.16	Number of beams with narrow beamwidths	67
5.17	Average number of switches with memoryless transmissions	69
5.18	Percentage decrease given by memory in DGS algorithm	69
5.19	Percentage decrease given by memory in EDP algorithm	70
5.20	Percentage decrease given by memory in random algorithm	70
5.21	Percentage of successful memory accesses with DGS algorithm	70
5.22	Percentage of successful memory accesses with EDP algorithm	71
5.23	Percentage of successful memory accesses with random algorithm	71
A.1	DGS switches with memory	77
A.2	EDP switches with memory	77
A.3	Successful memory attempts with DGS algorithm	78
A.4	Unsuccessful memory attempts with DGS algorithm	78

A.5	Successful memory attempts with EDP algorithm	78
A.6	Unsuccessful memory attempts with EDP algorithm	78
B.1	DGS switches with memory	79
B.2	EDP switches with memory	79
B.3	Successful memory attempts with DGS algorithm	79
B.4	Unsuccessful memory attempts with DGS algorithm	80
B.5	Successful memory attempts with EDP algorithm	80
B.6	Unsuccessful memory attempts with EDP algorithm	80
C.1	Successful memory attempts with DGS algorithm	81
C.2	Unsuccessful memory attempts with DGS algorithm	81
C.3	Successful memory attempts with EDP algorithm	81
C.4	Unsuccessful memory attempts with EDP algorithm	82
C.5	Successful memory attempts with random algorithm	82
C.6	Unsuccessful memory attempts with random algorithm	82
C.7	Average amount of saved switches for every memory access with DGS algorithm . . .	82
C.8	Average amount of saved switches for every successful memory access with DGS algorithm	82
C.9	Average amount of saved switches in each pattern with DGS algorithm	82
C.10	Average amount of saved switches for every memory access with EDP algorithm . . .	83
C.11	Average amount of saved switches for every successful memory access with EDP algorithm	83
C.12	Average amount of saved switches in each pattern with EDP algorithm	83
C.13	Average amount of saved switches for each memory access with random algorithm . .	83
C.14	Average amount of saved switches for every successful memory access with random algorithm	83
C.15	Average amount of saved switches in each pattern with random algorithm	83

INTRODUCTION

The evolution in the mobile communication field is going towards the definition of the 5G standard, which includes a larger set of applications in addition to the traditional services. The requirements of a subset of the use-cases can be fulfilled by an improvement of current mobile systems. Conversely, the larger relevance of high-rate and low-latency applications is leading towards the utilization of higher frequency transmissions. In particular, researchers and network operators are going beyond UHF frequencies and focusing on 60 GHz millimeter-waves (mm-waves) communications, able to guarantee remarkably better performances in terms of capacity as well as the possibility of an unlicensed exploitation of such frequency band.

However, mm-waves communications are heavily affected by higher path loss and obstacle attenuation, as well as a larger conditioning by the presence of physical elements in the propagation environment. Moreover, propagation features limit their use to Line-Of-Sight (LOS) and low-order reflected transmissions, which imply a radical change of communication mechanisms. The drawback of the higher path loss can be compensated for by the application of beamforming techniques that focus the energy towards specific directions. The use of narrow beams helps to achieve suitable transmissions, as it allows covering typical propagation distances. However, these features obstruct the exclusive utilization of mm-waves, as they cannot provide a continuous coverage and their use is limited to short-range small cells.

In order to guarantee a reliable service, the maintenance of a legacy network, based on lower frequencies, is required, in particular related to the exchange of signaling messages. A multi-layer HetNet represent a valid solution, able to combine the better coverage of a macrocell with the higher capacity of small cells. In order to exploit the features of both cell typologies, the network architecture proposed in the MiWEBA project is based on a functional split between U-plane and C-plane. The signaling messages exchange will be managed by legacy communication network, able to guarantee a more reliable service as it is less affected by the propagation drawbacks of

mm-waves, which conversely are limited to data transmissions.

The utilization of small cells is based on a connection establishment between a User Equipment (UE) and a mm-wave BS. The features of beamforming techniques hinder the cell discovery procedure, as the utilization of narrow beams implies that both UE and BS are required to beam out each other in order to begin the synchronization procedures needed for the association phase. Consequently, the use of unsuitable beams can result in a remarkable delay, due to the large amount of available antenna configurations.

In this work, we analyze the behavior of three algorithms that define an antenna configuration sequence to be used for cell discovery. The cell search procedure is supported by an external localization service, which allows obtaining information about the MS position. Such information will be provided from the MS to the macro cell BS exploiting legacy communication network, with the aim of assisting the evaluation of a proper antenna configuration and reducing the time needed for the procedure. The performances of the algorithms are compared by using several propagation scenarios with different characteristics in terms of accuracy of the localization information and impact of possible obstacles in the environment. Moreover, we introduce the concept of learning memory procedure, able to exploit the information about previous connections in order to successfully assist the procedure and further reduce the delay.

This thesis work is organized as follows: Chapter 2 introduces the main characteristics and reasons that led to the definition of 5G standard. In Chapter 3 the significant aspects of the propagation with millimeter waves are highlighted, as well as a description of the most relevant architectural solutions that will characterize mm-wave access networks. Chapter 4 provides a detailed description of the algorithms used to define configuration sequences to be exploited during the cell search procedure, in addition to introducing the concept of learning memory. Chapter 5 focuses on the numerical results obtained from Matlab simulations, while eventually Chapter 6 contains the conclusions of this thesis work, as well as suggestions for future works on this topic.

INTRODUCTION TO 5G STANDARD

This first Chapter is dedicated to a general description of 5G standard: Chapter 2.1 deals with an introduction and the reasons behind 5G standardization. In Chapters 2.2 the main requirements of 5G networks are listed. Chapter 2.3 contains a description of the main service types, as well as an introduction to the concept of SDN and NFV. Eventually, Chapter 2.4 explains some significant reasons that led to the choice of mm-waves.

2.1 5G overview

In the last few years, high-speed mobile connectivity is becoming one of the main topics in telecommunication field. An Internet connection is now a basic requirement in common life and network providers have to fulfill this need, that will become increasingly important in the next years, when Internet will be related to a greater number of aspects. Technologies that today are at the dawn, as wearable devices, and others that are still being studied, such as self-driving cars, will represent an important aspect of life in a few years. Moreover, it cannot be overlooked the impact of the Internet of Things (IoT), enabling the possibility to connect to Internet a greater number of devices, in addition to the objective of the creation of smart cities, which represent a model of city environment entirely connected in order to improve its efficiency. Today's infrastructures and technologies will not be able to handle these requirements, therefore a new standard is going to be established, commonly known as 5G and defined by NGMN Alliance as an end-to-end ecosystem to enable a fully mobile and connected society [1].

The number of mobile subscriptions is becoming bigger and bigger, in addition to the amount of data each device needs. The following Tables, taken from [2], offer a forecast of the devices spread and their data requirements in the next years and show how an increase of the number of devices is combined with a growth of the traffic:

Mobile subscriptions	2014	2015	2021 forecast	CAGR 2015-2021	unit
Worldwide mobile	7.100	7.400	9.100	5%	million
Smartphone	2.600	3.400	6.400	10%	million
Mobile broadband	2.900	3.600	7.700	15%	million
Mobile PC, tablet and mobile router	250	250	350	5%	million
Mobile, GSM/EDGE-only	4.000	3.600	1.300	-15%	million
Mobile, WCDMA/HSPA	1.900	2.200	3.200	5%	million
Mobile, LTE	500	1.000	4.100	25%	million
Mobile, 5G	-	-	150	-	million

Table 2.1: Mobile subscription essentials

Traffic essentials	2014	2015	2021 forecast	CAGR 2015-2021	unit
Monthly data traffic per smartphone	1.0	1.4	8.5	35%	GB/month
Monthly data traffic per mobile PC	4.0	5.8	20	25%	GB/month
Monthly data traffic per tablet	1.8	2.6	9.7	25%	GB/month
Total monthly mobile data traffic	3.2	5.3	51	45%	EB/month
Total monthly fixed data traffic	50	60	150	20%	EB/month

Table 2.2: Traffic essentials

Other kinds of devices, such as tablets, laptops and sensors, will require an Internet connection, and a common view expects 50 billion devices and objects connected to Internet in 2020 [3], even if more conservative evaluations estimate a value of 28 billion [2].

Future systems should be able to support up to 100 times more devices than today, leading to the necessity to support massive capacity and connectivity even in crowded areas. The spread of various typologies of devices, each characterized by different requirements in terms of setup time, latency, energy consumption and data amount, requires 5G networks to provide support for an increasingly various set of services, applications and use cases exploiting a single RAN network, in order to be an economically suitable solution [4]. The availability of a general wireless connectivity will be alongside the extension and the enrichment of traditional wireless services. The possibility to collect information from the environment will enable the application of improved systems in transportation field, allowing exploiting traffic information in order to offer a better travel experience. Moreover, sensors will introduce the possibility to improve people's healthcare and enable remote operations and controls, and their deployment must be able to support a considerable number of simultaneous connections.

The performances required by 5G networks will be remarkably greater with respect to current networks, and different techniques can be employed to achieve this goal. Network densification, based on hotspot addition, will require a cost-efficient deployment, while spectrum extension will ensure an efficient use of higher spectrum bands, with the exploitation of cooperative access technologies. User perception should be improved, with the goal of 100% of coverage and 99.999% of availability. A comparison between technical objectives of 4G and 5G networks is shown in Figure 2.1:

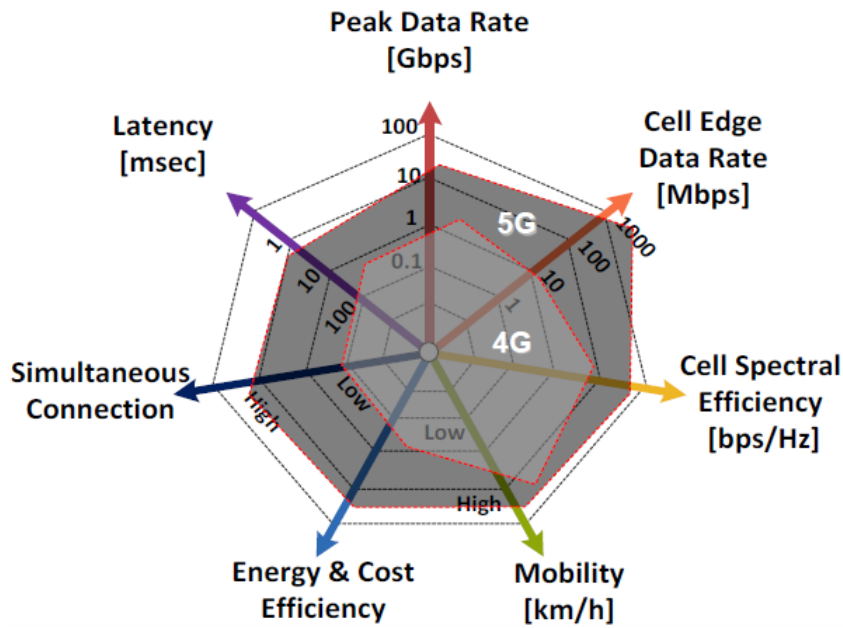


Figure 2.1: Differences between 4G and 5G technical objectives

2.2 5G main requirements

From the user's point of view, the transition to 5G networks will deeply positively affect the mobile experience. Figure 2.2 shows a comparison between rates offered by different generations of mobile communications:

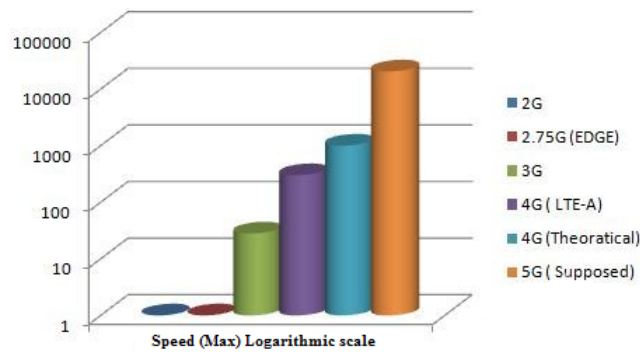


Figure 2.2: Comparison between rates in mobile communication generations

LTE Advanced is today's most advanced technology in cellular systems and can offer a downlink rate of 300 Mbps per user, with the possibility to apply carrier aggregation techniques and reach a peak rate of 1.5 Gbps with the exploitation of five different carriers [5]. The goal of 5G networks will be to supply a 10 Gbps download peak rate [6], while ensuring a 1 Gbps uniform coverage [7].

A significant improvement topic is related to energy consumption, as mobile phones, sensors

and other devices in the IoT field need to be battery-equipped, so the extension of the battery duration will result in a longer lifetime, with the goal of a 10-year duration [8]. The developments are going towards the evolution in battery technology and the improvement of the conditions in which devices work, in order to reduce their energy consumption. Some strategies can help in achieving this goal and extending battery lifetime. The solution proposed in [9] is based on the exploitation of the TDD frame structure in order to reduce the activity time of a device and keep it in an energy-saving mode for the majority of the time. Another factor that leads to the necessity of a battery extension is the power consumption in the analog-to-digital (A/D) conversion. Power consumption is linearly proportional to the sampling rate and scales exponentially in the number of bits per samples [10] [11], preventing a high-resolution quantization at wide bandwidths for low-power devices with a large number of antennas [12]. Moreover, as a consequence of the utilization of several antenna arrays on 5G devices, a small improvement on a single antenna can result in a great boost on final outcomes. This aspect can be seen from a larger point of view as a part of a reduction of the network energy usage, coming from both an ecological goal and the purpose of a lowering of the impact of network OPEX [13].

5G networks must satisfy a more stringent requirement related to the latency. Figure 2.3 shows a comparison between latency times in different mobile communication generations:

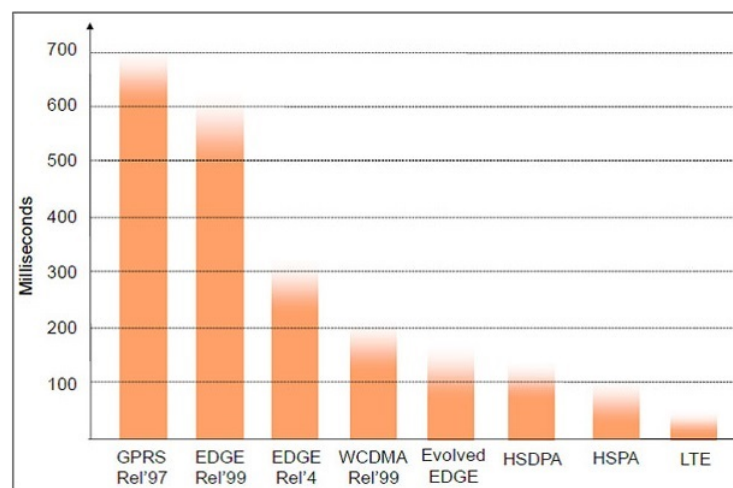


Figure 2.3: Latency times comparison

Even if LTE Advanced may reach a latency peak of 5 ms in the user plane [14], this value may be too high for some applications. Scenarios such as self-driving cars and systems that replicate natural human interaction with the environment need a latency even smaller than 1 ms. The ultimate goal is to reach the so-called Zero latency condition [15], in which latency is still greater than zero, but it's so low that the radio interface will not be the bottleneck. Even if next years will be characterized by a remarkable progress in processor speeds and network latency, physical limits must be respected, so services requiring less than 1 ms latency time need

their contents to be stored in a physical location very close to the user's device. A valid solution locates contents at the base of the cells, however it would cause an increase in CAPEX spent on infrastructures for content distribution and servers. Moreover, if a service requires 1 ms delay and an interconnection between operators, this interconnectivity must also occur very close to the physical location of the users. This requires an interconnection point at every base station, thus impacting the topological structure of the core network. A valid solution is the implementation of a single network infrastructure and only one radio network, which will be utilized and shared by all operators. Such a model would substantially reduce CAPEX in the network build, as only a single network would be built, but would require remarkable levels of cooperation between operators [13].

The need of improved performances with respect to current mobile standards leads to a set of remarkable modifications related to several transmission aspects. The higher data rate required can be partly obtained by the exploitation of a higher spectral efficiency. LTE can reach a spectral efficiency of $4.08 \frac{bps}{Hz}$ for a SISO channel and $16.32 \frac{bps}{Hz}$ for a 4x4 MIMO channel, while LTE-Advanced can reach $3.75 \frac{bps}{Hz}$ for a SISO channel and $30 \frac{bps}{Hz}$ for an 8x8 MIMO channel [16]. The application of MIMO technology in 5G standard may allow improving these results, exploiting the greater number of small antenna elements that will be incorporated on 5G devices and multi-user spatial multiplexing techniques.

Economic reasons are pushing towards the goal of lower deployment and infrastructural costs, due to the possibility to create small coverage cells by using low powerage BSs. This aspect has gained a major importance as one of the main drawbacks in today's mobile communication networks, in particular related to LTE coverage, is that the expansion of macro-networks implies the deployment of more expensive macro-eNBs, while finding new macro-sites becomes more and more difficult. An alternative is represented by the addition of small cells exploiting low-power base stations to existing macrocells, due to an easier and cheaper site acquisition and a lower equipment's cost. In order to ensure dense coverage, BSs location must be able to provide LOS transmissions, as 5G networks will mostly require this kind of transmissions as described in Chapter 3. Traditional locations are still suitable, while new ones, such as lampposts or sides of buildings [17], will be introduced.

A solution based on different-size cells can be useful also in order to get better results in terms of versatility and scalability, in particular by using the concept of HetNet (Heterogeneous Network), namely a network composed of macrocells, microcells and femtocells [18], shown in Figure 2.4.

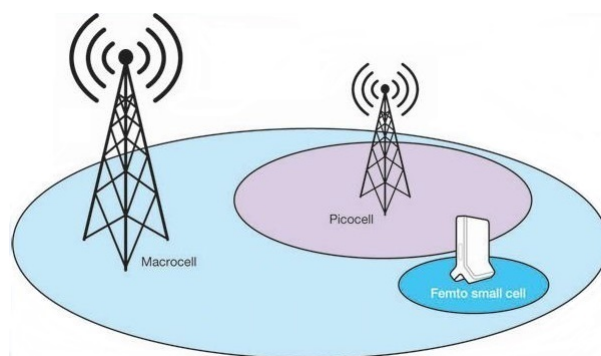


Figure 2.4: HetNet

A traditional network composed of macrocells can be upgraded by the installation of BSs to create additional high-capacity small cells in the zones that require a greater amount of traffic in order to increase their capacity, similarly to the concept of cell densification also seen in previous generations. Moreover, small cells can be used to fill in outdoor and indoor areas not covered by the macro network, allowing mobile operators to create a combination of pre-existing technologies, such as 2G, 3G, 4G and Wi-Fi, to ensure higher coverage and lower outage probability [13]. These small cells can increase the user rates and improve network performance and service quality by offloading user traffic.

As shown in Chapter 2.4, 5G communications will be characterized by the use of a much shorter wavelength with respect to current mobile standards, enabling the deployment of antenna arrays with a large number of small elements in the tiny space of the mobile devices, in order to exploit path diversity, especially when LOS transmissions are blocked, and reduce the impact of human obstructions [19]. A single antenna element will not satisfy the gain requirements of several applications, therefore antenna arrays are particularly interesting since they are able to offer sufficiently high gain. The authors in [20] consider how the use of a phased-array antenna configuration would increase the link budget, due to the phased-array gain and the possibility to increase the transmitted power, with a contribution equal to $10 \cdot \log_{10}(N_{TX}^2 \cdot N_{RX})$ dB, where N_{TX} and N_{RX} are respectively the elements of the configuration in transmission and reception.

Despite the advantage just presented coming from the use of a fixed antenna array, a different architecture has been introduced. A very critical aspect is the antenna capability to align its narrow beam towards the direction of the strongest signal, especially in mobile applications, therefore a beam-steerable antenna array solution should be considered. The solution proposed in [21] and [22] consists of the integration of all array electronics in a single chip, however this architecture presents a fixed number of antenna elements, so it does not guarantee good levels of flexibility, in addition to drawbacks related to production cost, heat dissipation, feed circuitry complexity and losses in the feeding lines that limit the number of elements in the array [23]. An improvement is represented by the Modular Antenna Array (MAA) architecture proposed in [24], composed of several low-cost mm-wave front-end sub-array modules. Each antenna element

can be provided with the desired amplitude and phase distribution by means of on-chip phase shifters and variable gain amplifiers, and therefore is capable of independent beamsteering. All antenna modules are connected to the central beamforming unit implemented in the baseband, able to refine the coarse beamforming provided by the modules. Figure 2.5 shows a schematic diagram for Modular Antenna Array architecture:

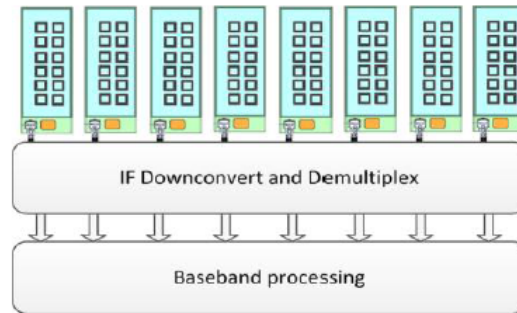


Figure 2.5: Modular Antenna Array architecture

An evolution of MAA architecture is the Full Adaptive Arrays (FAA) concept, in which each antenna element can process its signals independently by exploiting its RF chain. The advantages are related to the increase of the number of the degrees of freedom, now equal to the number of antenna elements, and the lack of limitations in beamforming in both vertical and horizontal planes in a two-dimensional architecture. FAA can help in achieving improved results in the case of groups of users in MU-MIMO mode, as constraints in degrees of freedom curb MAA in beamforming with maximal gains towards arbitrary group of users, while both architectures would obtain the same performances in single-user mode [17].

2.3 5G application scenarios

The possibility to provide connectivity to a larger set of applications enables 5G networks to embrace several new scenarios. In particular, a deep analysis performed by METIS project allows identifying three main service types, each characterized by specific requirements in terms of coverage and data rate [25]:

- Extreme Mobile BroadBand (xMBB) requires extremely high data rates for high-demand applications, such as augmented reality or remote presence [26]. Moreover, low-latency communications can provide a connection experience without perceived delays, in addition to a reliable broadband access over large coverage areas even in crowded environments. This allows guaranteeing satisfactory levels of performances during large public events by improving the Quality of Experience in terms of latency and data rate per user.

- Massive Machine-Type Communications (mMTC) will be used for the billions of battery-equipped devices that will require a connection, and typical applications are related to environmental controls and monitoring tasks. The main challenge is related to the necessity to employ a single communication network to serve various typologies of devices characterized by different degrees of complexity and requirements, in addition to the burden of the large overhead needed to manage such amount of devices. Key priorities are scalable connectivity for an increasing number of devices per cell, wide area coverage, deep indoor penetration and low cost and complexity.
- Ultra-reliable Machine-Type Communications (uMTC) are mostly related to safety and time-critical applications [27]. A possible application is vehicle to anything (V2X) communication, able to provide high levels of service experience to moving end-users, where the main priorities are related to the mobility management and the necessity of a robust and highly reliable connectivity able to provide low-latency communications. As far as M2M (Machine-to-Machine) communications for industrial applications are concerned, requirements are mostly related to safety and control features in terms of reliability and availability.

The management of such complex networks can be handled by software applications, with the exploitation of a flexible architecture based on emerging technologies such as Network Functions Virtualization (NFV) and Software Defined Networking (SDN). NFV is a network architecture concept that allows the separation of hardware from software, enabling network functionalities to be managed through software applications based on virtualization technologies that are executed on Virtual Machines on a single or more physical server. SDN is an extension of NFV technology that allows a dynamic reconfiguration of the network topology via software. This allows for example directing properly additional network capacity where needed in order to keep satisfactory levels of customer experience quality. The main advantages of such technologies are the optimization of the resource usage, the increase of the availability and a higher degree of flexibility.

2.4 5G spectrum opportunities

The analysis just exposed shows how the possibility to provide connectivity to a large set of different applications leads to the necessity of the adoption of multiple transmission frequencies, in order to properly fit the features of each service. While MTC requirements are mostly related to coverage, so frequencies in the UHF band can be properly used for this purpose due to their more appropriate coverage properties, conversely xMBB requires an extremely high data rate to fulfill the needs described earlier in terms of traffic. Furthermore, the forecast about the growth of data traffic in the next few years emphasizes the necessity to find a solution to prevent system capacity shortage. A solution to the spectrum scarcity may be the transition from lower frequencies to higher spectrum bands, which are more appropriate to fulfill such capacity requirements. The idea

is to move beyond 6 GHz and exploit the so-called millimeter waves (mm-waves), electromagnetic waves with frequencies in the order of tens of GHz, in particular between 30 and 300 GHz. Figure 2.6 shows a representation of the main frequency bands between 2 and 90 GHz:

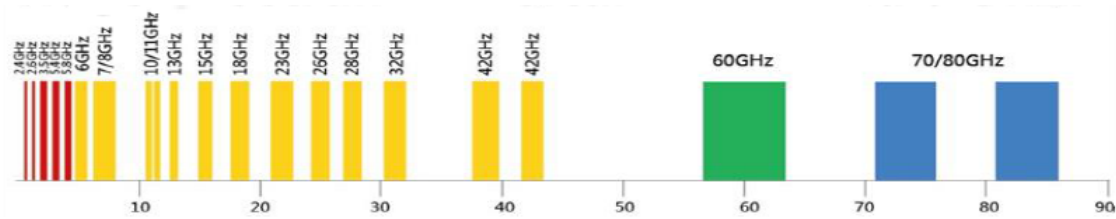


Figure 2.6: Main frequency bands for wireless communications between 2 and 90 GHz

Preliminary studies prove how higher frequencies can represent a valid solution for mobile communications. The authors in [28] found interesting reflection and penetration properties for a 28 GHz transmission in an urban environment, while [29] proves the viability of a 73 GHz transmission. Among all the available spectrum zones, a considerable interest is reserved to the 60 GHz unlicensed band, between 57 and 66 GHz, and the light-licensed E band, between 71 and 76 GHz and between 81 and 86 GHz. Nowadays, different zones of the spectrum are still under consideration in order to be chosen for 5G transmissions, by the way the bandwidth around 60 GHz has a great potential to play that role, as worldwide it presents a good portion available for this aim. Figure 2.7 shows the different available zones around 60 GHz in several countries:

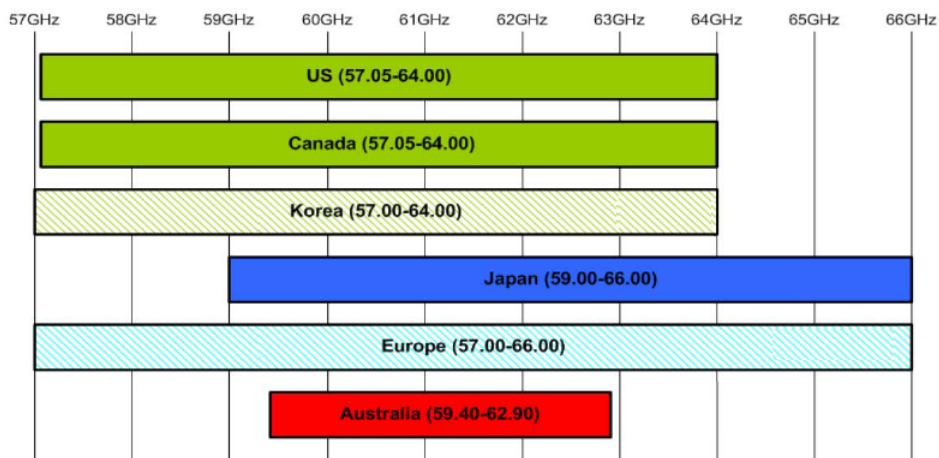


Figure 2.7: Spectra available around 60 GHz

MM-WAVE ACCESS NETWORKS

In this chapter we deal with the features of 5G standard related to mm-wave access networks. Chapter 3.1 considers the concept of HetNet. In Chapter 3.2 the main features of mm-waves transmissions are exposed. Chapter 3.3 is used to illustrate a general overview about beamforming techniques. Chapter 3.4 is dedicated to a description of the new architectures that will be exploited in 5G networks, focusing on U/C-plane splitting and C-RAN, while in Chapter 3.5 an analysis of cell discovery mechanisms is performed.

3.1 HetNet

A solution to fulfill the different requirements of 5G networks is related to the concept of HetNet introduced in Chapter 2.2, based on a multi-layer network architecture. A network composed of macrocells and microcells can be a valid solution, if advantages of both cell typologies, respectively the universal coverage and the higher available rate due to the exploitation of beamforming techniques, can be exploited. Differences between cells are not only related to their sizes, as microcells are used to offer LOS transmissions, due to the mm-waves high penetration attenuation, while macrocells exploit lower frequency propagations and therefore are able to guarantee an adequate coverage even in NLOS conditions.

5G networks will be innately heterogeneous, as the exclusive exploitation of mm-wave communications is not able to provide a uniform coverage and consequently to supply a reliable service, therefore a legacy network, based for example on LTE technology, is required. Heterogeneous networks are exploiting since GSM technology, where different frequencies are used to separate different-size cells [30]. Transmissions on multiple frequencies are still an available solution in LTE networks, however they are mainly characterized by the reuse of a single frequency, in order to maximize the utilization of the licensed bandwidth, so, in the conventional single-band HetNet

architecture, the same band is used both for the macrocell BS and smallcell BSs. Accordingly, the single-band HetNet requires interference mitigation techniques between macrocells and smallcells, such as Partial Frequency Reuse (PFR) and Soft Frequency Reuse (SFR), that allow mitigating the intercell interference (ICI) and improving performances in terms of throughput and spectral efficiency [31]. However, these techniques split the available bandwidth in different subbands and imply the presence of channelization loss.

5G standard introduces a different model for HetNet networks, in which macro and smallcell BSs use different frequency bands. The standardization of multi-band HetNet with inter-site carrier aggregation capability allows neglecting macro-smallcell interference control schemes. However, there are several drawbacks in the multi-band HetNet: first of all, there is a downside related to coverage, since smallcell BSs, operating at a higher frequency band with respect to macro BSs, can guarantee a scattered and not continuous coverage in the macrocell. Moreover, user devices must support dual connectivity for the two different bands, and their power consumption must be taken into account, as the cell search process done performed by UEs connected to the macro BS to find a smallcell BS is expensive from the energy point of view. Eventually, a drawback related to the handover procedure arises, in particular to the impact of failures on the final results, as smallcell coverage is limited and therefore it is not effective to perform regular handover processes as in the conventional scenario of macro BSs with the aim of a seamless user experience. The presence of several cells in the HetNet scenario makes the management of the handover procedure more challenging [32], as the handover process is actually composed of several processes between the different cells of the HetNet and therefore even a failure in a single step would imply that the whole process fails. We can consider the example of handover between two macrocells, where the whole process can be subdivided in intracell, between cells of the same macrocell, and intercell handover, between cells of different macrocells. The first situation is easier to manage, as the macro BS remains the same, while in the latter the MS must first establish a connection with the new macro BS, and later a connection to a smallcell BS controlled by that macro BS.

A significant topic to be considered related to the planning of HetNet is that mmW communications will require cell selections and path switching at much faster rates than current cellular systems. As shown in Chapter 3.2, mmW signals are very susceptible to little variations in the propagation environment and even a small movement of the user can considerably modify the propagation conditions, leading to shadowing and intermittent communications. A possible solution to overcome this situation is the exploitation of carrier aggregation techniques, as the simultaneous connection to several BSs could provide path diversity, but requires support for path switching and scheduling in the network. Carrier aggregation must be designed in order to be compatible with earlier mobile generations to allow a better utilization of spectrum [33].

A second issue in the evolution of HetNets for mm-waves will be multi-operator support. Exclusive access with higher frequencies may result in low spectrum utilization efficiency [34],

as the large amount of available spectrum may not be fully utilized by a single operator. A more efficient use of the spectrum neglects exclusive rights to a bandwidth, conversely a dynamic use of the licensed spectrum can assure better results in terms of spectrum utilization, as a static division of resources is not the best solution to fit the dense and time-variant environments that will characterize future 5G scenarios [6]. Operators should therefore find a way to share the spectrum, with the possibility to exploit the so-called Co-Primary Shared Access model, where several operators agree on a joint use of their licensed spectrum. The most significant Co-Primary Shared Access techniques are Mutual Renting (MR) and Limited Spectrum Pool (LSP). In MR, frequency band is divided in blocks, to which single operators have exclusive access, even if there is the possibility for the licensed operator to rent part of the unused blocks to others, while agreements among parties can be established in order to manage access priority matters. In LSP, a group license is given to several operators to access to a fraction of the whole band in a shared way. Mutual agreements among operators allow exchanging shares of the band in order to manage traffic variable loads [35].

Given the possibility of having multiple operators on the same bandwidth, it would be better to exploit some kind of mechanism in order to offer a better service to final users. In particular, an external party may manage cells and provide roaming support: 5G networks will require a bigger number of roaming processes with respect to current networks, due to the well-known coverage properties of the cells. Due to the inherent properties of mm-wave transmissions, which are very dependent on the physical features of the propagation environment, it would be better for a mobile device to be connected to cells from different operators simultaneously, exploiting carrier aggregation techniques, in order to increase the probability to find obstacle-free paths and consequently decrease the outage probability. The spectrum sharing among multiple operators requires more sophisticated inter-cell interference coordination mechanisms.

3.2 Mm-waves main features

The use of frequencies in the mm-wave band leads to the necessity to face new propagation features, that have a lower impact or are even absent in current communication systems. The main drawback related to mm-waves is a remarkable increase of the isotropic path loss. Its impact can be evaluated from an adaptation of Friis transmission equation in a free space scenario, that defines the relationship between the received power P_r and the transmitted power P_t as

$$P_r = P_t \cdot G_r \cdot G_t \cdot \left(\frac{\lambda}{4\pi R} \right)^n \quad (3.1)$$

where G_r and G_t are the antenna gains of the transmitting and receiving antennas respectively, R is the distance between antennas, λ is the wavelength used in the transmission and n is equal to 2.1, as in [36]. Focusing only on the last term, it emerges how even a little increase of the

frequency results in a not negligible reduction of the received power as

$$P_r \propto \left(\frac{1}{f}\right)^{2.1} \quad (3.2)$$

The transition from the current mobile frequencies in UHF band to 60 GHz frequency would lead to a more than 100 times lower receiver power and extremely range-limited transmissions, unless a proper configuration of antenna gains.

Another factor that disadvantages propagation is atmospheric absorption. The main reason is related to the oxygen absorption, which has a great impact on transmissions, as shown in Figure 3.1:

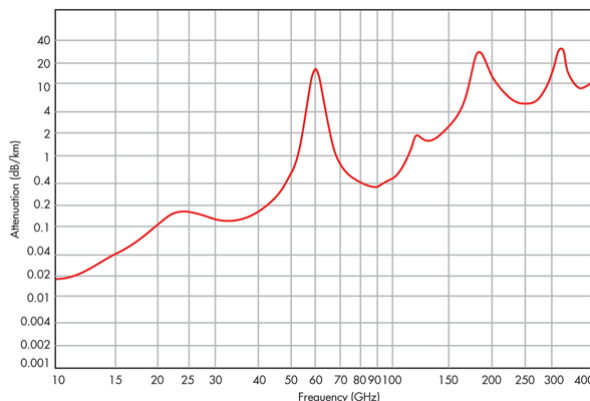


Figure 3.1: Signal attenuation at sea level and 20 °C versus log frequency

The absorption, caused by the interaction of electromagnetic waves with oxygen molecules, has its local peak around 60 GHz with a value equal to 20 dB/km, while is absent with frequencies lower than 10 GHz [37]. Moreover, transmissions at 60 GHz are quite influenced by rain attenuation, as raindrops are roughly the same size as the wavelength of the electromagnetic wave and can introduce scattering in radio signal transmission [33]. Figure 3.2 shows the relationship between frequency and rain attenuation varying the quantity of rain. There is a little but not negligible impact, not much greater with respect to current communication systems, because the distances at issue are not so large.

As a consequence of the transition from a few to tens of GHz frequencies, wavelengths will be in order of 1 cm and comparable with the majority of common objects. The propagation environment can therefore be considered as opaque, affecting in particular the aspects of propagation related to objects penetration and reflection. The opaqueness of the environment takes on greater significance because human body itself can heavily prevent transmissions, as it introduces an attenuation up to 20 dB [38]. Moreover, [39] shows the remarkable impact of pedestrians on an outdoor scenario, as they can temporarily block the UE-BS LOS connection and consequently extremely condition the received signal. Given the mm-waves drawbacks related to the objects penetration and a not significant propagation due to diffraction, in addition to a vastly reduction

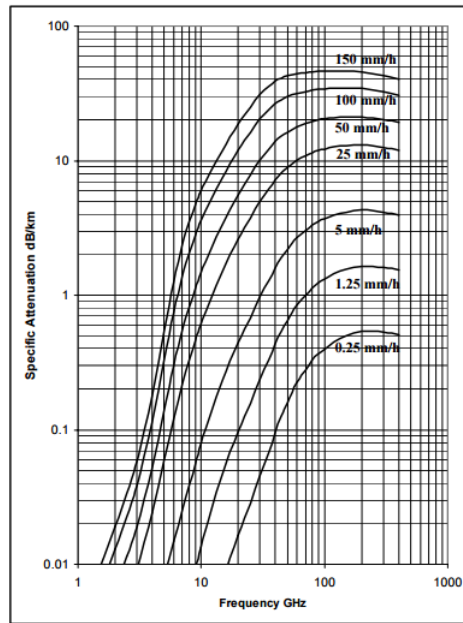


Figure 3.2: Rainfall attenuation vs frequency

of multipath effects mostly in outdoor environments [40], the main techniques to reach the receiver antennas are the exploitation of LOS transmissions or low-order reflected paths, that are very dependent on the material and the angle of arrival [41]. These propagation features may be the reason of shadowing phenomena, very common in both indoor and outdoor transmissions, as reflective surfaces can both promote and prevent propagation. Common elements, such as building walls, furniture and even human bodies, can be used as reflection surfaces in order to reach users in a NLOS condition, while in the meantime they can obstruct the reachability of a user located behind them leading to an outage situation. In a dynamic scenario, in which the elements in the environment are moving and accordingly the propagation conditions are continuously changing in time, the limited smallcell coverage makes connectivity highly intermittent, as an outage situation may arise due to a little variation in the environment or a user movement.

The increase of the transmission frequency leads to the necessity for the devices to operate faster, in order to better evaluate channel variations, due to the higher Doppler spread. By definition, it is proportional to the frequency carrier, therefore the transition to frequencies in the order to tens to GHz results in a small coherence time, that is inversely proportional to the Doppler spread [42]. This increases the probability of having a time selective channel and the consequent necessity of equalization at the receiver.

The use of 60 GHz transmissions will require remarkable efforts in preliminary studies, as mm-wave band is less studied with respect to traditional communication frequencies and there is still lack of channel measurements and modeling effort. Mm-waves represent a novelty in mobile communications, in addition to being a relatively new technology in WLAN systems too, as 60

GHz transmissions are exploited only since the recent 802.11ad version. Conversely, several standards are exploiting lower frequencies since early versions, so considerable standardization efforts have been already done. Moreover, 60 GHz transmissions are more difficult to be modeled, as several factors, such as traffic variations and propagation scenario, must be taken into account in order to derive an efficient model [17].

As far as propagation mechanisms are concerned, the polarization characteristics remarkably affect the received power. Authors in [43] found that the power degradation due to polarization characteristics mismatch between transmit and receive antennas can be up to 10-20 dB. The use of high directional steerable antennas implies that essentially only one component will be used for signal transmission, and even reflected signals remain polarized at the receiver. Moreover, the accurate polarization alignment required by linearly-polarized solutions is not very practical to be implemented for mobile devices [24]. Circular polarization is therefore seen to be a key requirement for 60 GHz wireless applications, as it can significantly increase the robustness of a communication link, by reducing multipath effects in LOS environments in the 60 GHz band, besides reducing channel delay spread and improving error performances for high-rate communications [44].

Moreover, nowadays there are several applications that make use of 60 GHz band: [45] shows a scenario with mobile backhaul exploiting mm-wave transmissions, while [46] considers the use of 802.11ad devices within LAN networks. However, all these mm-wave applications are characterized by point-to-point transmissions and the lack of simultaneous communications. Conversely, 5G networks will be characterized by the presence of several concurrent transmissions, in order to fulfill the requirements described in Chapter 2 and obtain better results in terms of spatial reuse and spectral efficiency. The contemporary presence of multiple links is therefore fundamental, but a potential interference among them arises, leading to the necessity to introduce mechanisms able to coordinate several transmissions.

Despite the drawbacks exposed so far, the adoption of frequencies in the 60 GHz band can result in various positive aspects, in addition to the ones described in Chapter 2. One of the main reasons behind the efforts in 5G standardization is certainly the necessity to increase data rate, and mm-waves can be a valid solution of achieve this goal. A prove of this availability can be obtained starting from Shannon's capacity theorem. The capacity C of a channel is given by the formula

$$C = B_w \cdot \log_2(1 + \gamma) \quad (3.3)$$

where B_w is the channel bandwidth and γ is the channel SNR, defined as $\frac{P}{N_0 \cdot B_w}$, where P is the received power and N_0 is the noise power spectral density [47]. Bandwidth is often expressed in terms of fractional bandwidth (FB), defined as the ratio between the bandwidth B_w and the center frequency f_0 of a signal [48], as FB is constant with respect to frequency. In wireless communication systems, coverage is defined with respect to a minimum SNR γ_0 , therefore, to

keep γ_0 constant, the corresponding received power P_0 should be a function of f_0 as follows:

$$P_0 = \gamma_0 \cdot N_0 \cdot B_w = \gamma_0 \cdot N_0 \cdot FB \cdot f_0 \quad (3.4)$$

The capacity C is therefore a function of the center frequency f_0 , so it can be improved by adopting a higher frequency.

The use of higher frequencies involves a minor impact of interference on transmissions. Nowadays communication systems are interference-limited, because inter-cell interference from neighboring cells is the dominant source of radio-link impairment, in particular in the case of highly traffic loaded smallcell deployments [49]. In addition to inter-cell interference, another factor to be considered is the intra-cell interference, coming from other transmissions within the same cell. This scenario is no longer suitable for 60 GHz communications, as higher path loss and oxygen absorption heavily attenuate mm-wave transmissions, limiting not only the distances they can cover, but also the interference effects among them, leading to an increase of the frequency reuse [50]. In addition, a further decrease of the interference impact is caused by the smaller transmission beamwidth with respect to current mobile communication systems. Nevertheless, mostly in indoor scenarios [51], interference effects cannot be neglected at all. One of the main techniques to counteract interference and improve network capacity is the concept of spatial reuse, namely the ability of the network to support concurrent transmissions in the same neighborhood without interfering with each other.

Even if mm-wave band has never been used in cellular networks, nowadays there are several wireless systems that exploit 60 GHz transmission band. In addition to the ones described earlier, [52] shows the use of mm-waves in battlefield communications, while [53] deals with a millimeter wave scanner. One of the most interesting uses is WiFi transmission: the current latest version is the 802.11ad WiGig standard, able to provide up to 6.75 Gbps throughput using approximately 2 GHz of spectrum at 60 GHz, while the future version, called 802.11ay, should be able to offer a 20 Gbps throughput [54]. The spread of such popular technologies can indirectly be useful also for the exploitation of 60 GHz band for mobile communications, as it contributes to an advance in CMOS RF technology in order to enable low-cost mmW chips suitable for mobiles devices [12]. Moreover, despite the shortage of dedicated studies in the mobile communication field, the features of wireless communications more strictly related to the propagation are independent of the specific application, therefore some general studies and researches about these topics in the context of 802.11ad standard can be reused also in the cellular network field and operate as starting point for specific and more focused studies.

Furthermore, the features of 60 GHz transmissions allow increasing the security level. Both small beam sizes and oxygen absorption, by limiting the effects of interference, can help in obtaining more harmless communications, as a link will not interfere with another one in the immediate vicinity if their paths are just slightly different, while oxygen absorption enables to avoid that the signal propagates far beyond the target antenna. In order to intercept the signal, an attacker would have to put an intercepting receiver, which has to be tuned to the carrier signal

of the transmitting radio and be in the main beam, on the same trajectory and very close to the target. The presence of the intercepting device would degrade the path of the transmitting radio and jam its receive path, so it would be unlikely that the attacker could actually obtain data and stay undetected.

Eventually, as transmission power is mostly propagated between the transmitting and the receiving antennas through LOS or low-order reflected paths, the behavior of the propagated beams can be considered as quasi-optical. A consequence of this kind of propagation nature is that image based ray tracing can be efficaciously used for predictions of the channel paths and to assist the channel modeling [55], enabling the possibility to run simulations even without physical measurements. However, even if the exclusive application of ray tracing simulations can accurately predict the propagation paths, this approach doesn't exclude the possibility to integrate and verify theoretical measurements with practical data obtained from measurement campaigns.

3.3 Directional transmissions

The use of mm-waves introduces a trade-off between data rate and coverage, as Equations 3.3 and 3.4 show that data rate can be increased by the use of a higher frequency, while conversely [20] proves that the coverage is inversely proportional to the frequency. Despite the outstanding advantages coming from the use of higher frequencies, however the remarkable impact of the path loss on transmission features cannot be neglected. Friis transmission equation indicated in Equation 3.1 shows that an easy way to counteract the higher path loss is the exploitation of transmitting and receiving gains. The idea is to use high-gain directional antenna arrays, going away from the traditional omnidirectional antenna model suitable for previous generations, as millimeter waves allow exploiting a very small range for antenna size and spacing. This technique enables the possibility to have a directional transmission or reception, combining elements in a phased array in such a way that signals can experience constructive or destructive interference according to the angles, in order to focus the energy towards specific directions and propagate further. The effectiveness of this procedure can be proved starting from Equation 3.2, where the use of 60 GHz frequency would introduce a supplementary path loss of over 27 dB with respect to 2.6 GHz LTE transmissions. The authors in [56], exploiting an antenna array with 16 elements at both transmitter and receiver, show a link budget gain equal to 24 dB, able to almost compensate for the effects of the higher path loss. Consequently, mm-wave propagation, with an appropriate beamforming, may be characterized by slightly lower performances with respect to current mobile frequencies.

The effective use of beamforming technique is complicated by the features of the environment in which communications take place. A real scenario is characterized by a great number of concurrent transmissions between mm-wave APs and MSs, so a remarkable coordination effort

among transmissions is fundamental, in order to fully cover the whole environment and guarantee a good experience to users even in densely populated networks in terms of fairness, outage rate and number of supported devices. These requirements further complicate the beamforming of such transmissions, because it requires the knowledge of the best beams before every decision of coordinated transmissions, in order to maximize the total system capacity [57]. Moreover, the short coverage of mm-wave APs hinders the effective applications of beamforming techniques, as it requires additional and more frequent efforts for seamless handover.

3.4 Advanced network architectures

The features of mm-waves require innovative network architectures in order to be profitably used in the access networks. In particular, the U/C-plane splitting and the C-RAN represent interesting solutions to be used in mm-wave scenarios and will be described in the next sections.

3.4.1 Control and user plane separation

As described earlier dealing with the concept of multi-band HetNet, future 5G networks will be characterized by the presence of macrocells and smallcells. A reasonable idea is to combine the inherent features of both topologies in order to exploit the consequent properties, where macrocells can be used to guarantee coverage, as lower frequencies can ensure a better propagation against obstacles and path loss, while smallcells will provide extremely high data rates and offloading in zones with a huge traffic concentration. The intermittent coverage of smallcells can however prevent the fulfillment of a reliable service, in particular as far as signaling messages are concerned. The network architecture proposed in the MiWEBA (Millimeter-Wave Evolution for Backhaul and Access) project can help to overcome this issue, as it is based on a functional split between user (U) and control (C) plane, where the latter will be managed through macrocells communications, by the exchange of signaling messages between UEs and BS exploiting legacy transmission technology, while higher frequencies and smallcells can be used to offer high capacity transmissions to users. Figure 3.3 shows the proposed architecture for 5G mobile networks.

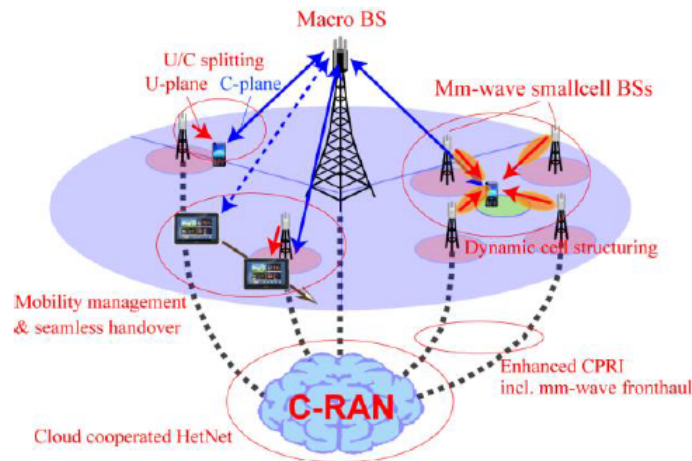


Figure 3.3: Proposed architecture for 5G cellular networks

Macrocells are standard cells as they support both C-plane and U-plane signaling, while smallcells are used only to carry user traffic. As they are not configured with cell-specific signals, smallcells are called phantom cells [58]. U/C-plane splitting emphasizes the differences between the BS typologies, as connectivity is guaranteed by macro BSs working on C-plane, enabling a centralized management of UEs mobility and traffic in the HetNet and consequently facilitating the UEs cell discovery, due to the management of the connection procedure between UEs and smallcell BSs. Conversely, smallcell BSs work only on U-plane in order to provide high data rate. For this reason, the increase of the capacity is easy to be managed, as it's enough to deploy additional smallcell BSs where needed, leading to good performances in terms of scalability. Moreover, the remarkably larger coverage of macrocells with respect to phantom cells implies that the amount of handover in the C-plane is lower compared to the standard coupled HetNet architecture. In a single macrocell, the handover process is reduced to a U-plane handover and therefore lots of control signaling interaction can be saved [59].

3.4.2 C-RAN solutions

Alongside U/C-plane splitting, the C-RAN (Centralized or Cloud Radio Access Network) paradigm can help to overcome the standard HetNet drawbacks. The traditional concept of BS is composed of RRH (Radio Remote Head) and BBU (Baseband Unit) parts physically close, where the first is dedicated to the radio functions of the transmission, including amplification, up/down conversion, filtering, A/D and D/A conversion, while BBU pool is used for processing tasks. C-RAN architecture moves away from this model and represents a system of multiple RRH elements and a single centralized point, namely a farm of baseband processing nodes, responsible for all of the BBU processing tasks, to which the elements are connected exploiting using high bandwidth links. Figure 3.4 shows an overview of the C-RAN architecture, in which three main elements, i.e. the RRHs, the BBU pool and the fronthaul network, can be identified.

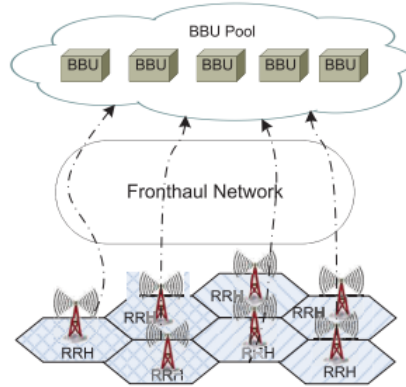


Figure 3.4: C-RAN architecture model

As described earlier, the RRHs are related to the radio tasks of the transmission, so they are responsible of the RF signals downlink to MSs and the baseband signals uplink from MSs to the BBU pool for further processing. The majority of the signal processing functions are now executed in the BBU pool, so RRHs can be relatively simple and can be installed in large scale scenarios and distributed in a cost-efficient manner [60].

The BBU pool is composed of BBUs which operate as virtual BSs in order to process baseband signals and optimize the network resource allocation. The concept of virtualization introduces the possibility to allocate processing capacity in a dynamic way by means of a centralized real-time adaptation technology. The BBU assignment for each RRH can be centralized or distributed, according to the resource management in BBU pool. In addition, different demands on network performance and system complexity must be considered too. In a distributed manner, there is a one-to-one correspondence between RRHs and BBUs, as each RRH is directly connected to its exclusive BBU. This model is characterized by an easy deployment, but it does not exploit the advantages of joint signal processing and central controlling in C-RAN [61]. Conversely, in the centralized manner, all the RRHs may be connected to a switcher device, which flexibly and dynamically schedules processing resources in BBU pool for a single or more RRHs, as shown in Figure 3.5.

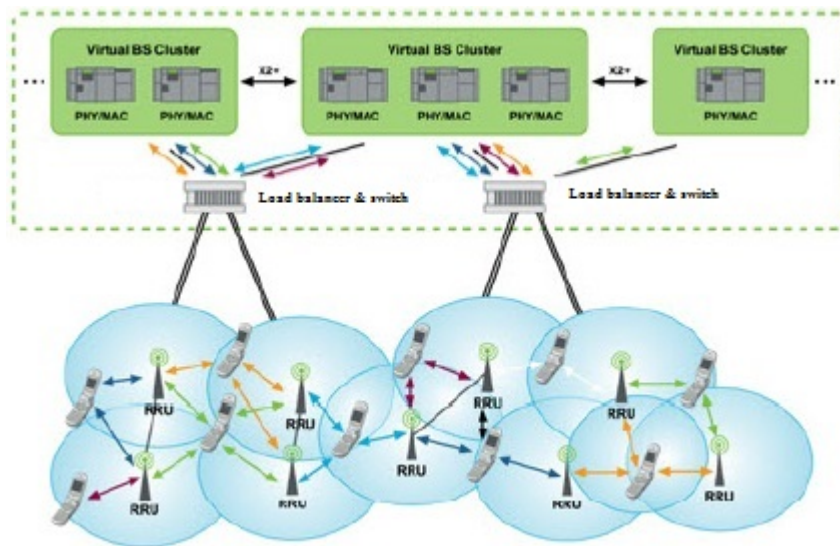


Figure 3.5: C-RAN centralized model

The advantages are related to flexibility in resource sharing, energy efficiency by joint scheduling and load balancing, while centralized processing allows implementing avoidance and cancellation interference algorithms and enables the possibility to selectively turn RRHs on/off dynamically according to the traffic variations. Within the centralized model, a further subdivision can be introduced, according to the location of baseband processing, therefore fully centralized and partial centralized architectures can be taken into account. Figure 3.6 shows the functional differences between the two architectures, respectively indicated as Solution 1 and Solution 2:

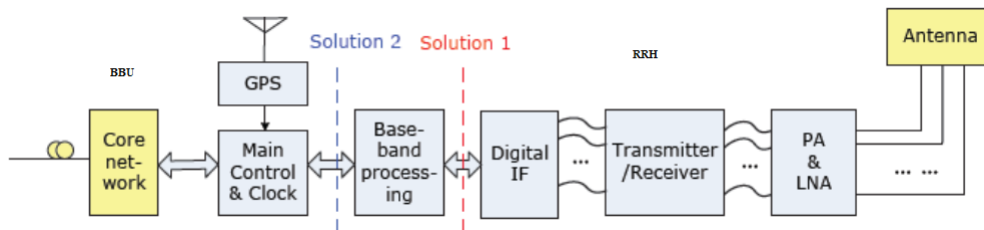


Figure 3.6: Fully centralized and partial centralized architectures

In the fully centralized architecture, BBU pool is responsible for baseband processing, allowing easy upgrades and capacity expansion and ensuring maximum resource sharing, but high-bandwidth BBU-RRH links are required. Conversely, the partial centralized architecture keeps the baseband processing into RRH tasks, requiring less bandwidth for RRH-BBU links, at the price of harder upgrades and less flexibility with respect to the fully centralized one, therefore the first scheme represents a better solution.

The fronthaul network, needed for the connections between RRHs and BBU pool, is composed of links that can be realized by using different technologies, exploiting for example optical and wireless links. An optical singlemode fiber, using a standard interface with a digital radio signal such as CPRI (Common Public Radio Interface) or OBSAI (Open BS Architecture Initiative), is a valid solution [62]. An optical solution is more complex to be installed with respect to a wireless one, however the use of a fiber is very convenient, as an optical link can help in reducing the coaxial feed line losses, given the lower attenuation described in [63], increasing system efficiency and providing a high level of flexibility in cell site construction. In addition, it provides large bandwidth and high data rate: for example, the NG-PON2 standard is able to provide a data rate of 40 and 10 Gbps for the downstream and upstream respectively [64]. Conversely, wireless links are faster and cheaper to be deployed than fiber, employing the microwave technology with carrier frequencies between 5 and 40 GHz, however they are characterized by a limited available bandwidth and can provide data rates in the order of a few hundred Mbps. Optical links are more helpful for this purpose and therefore represent a better solution.

3.4.3 Green networking solutions

The separation between functional entities will result in various positive aspects. As described above, the separation between radio and processing functions is no more only logical, but also physical, due to the different locations of RRHs and BBU. This splitting introduces the possibility of having modules that are dedicated only to a subgroup of tasks and consequently have much less energy consumption and complexity, contributing to a reduction of the total price, which has a great impact on the whole process, because power consumption represents a not negligible fraction of the total costs. An example, taken from [65], is shown in Figure 3.7, where the components of the power consumption of China Mobile are represented:

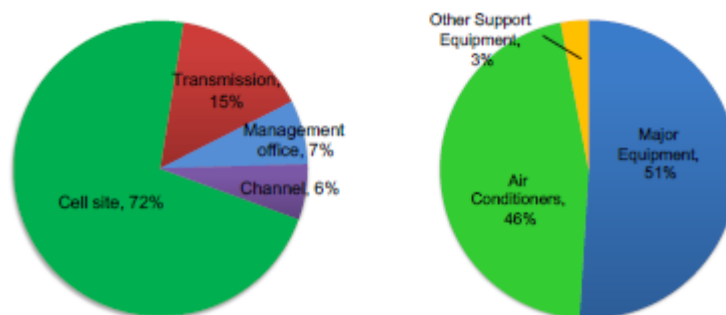


Figure 3.7: Components of the power consumption of China Mobile

In addition, as an easy method to increase network coverage is the deployment of new BSs, but this will result in a total cost increase, the possibility to compensate for the additional costs with the reduction of the power consumption expenses is a profitable way for network operators.

Moreover, in current RAN architecture, the processing capacity of each BS can only be used for its own MSs, without the possibility to share it with others in a larger area [66]. C-RAN concept will remove this limitation, allowing low-cost operations and profitable results in different scenarios. For example, traffic concentrations in residential or commercial zones are very time dependent in the daytime, as shown in Figure 3.8:

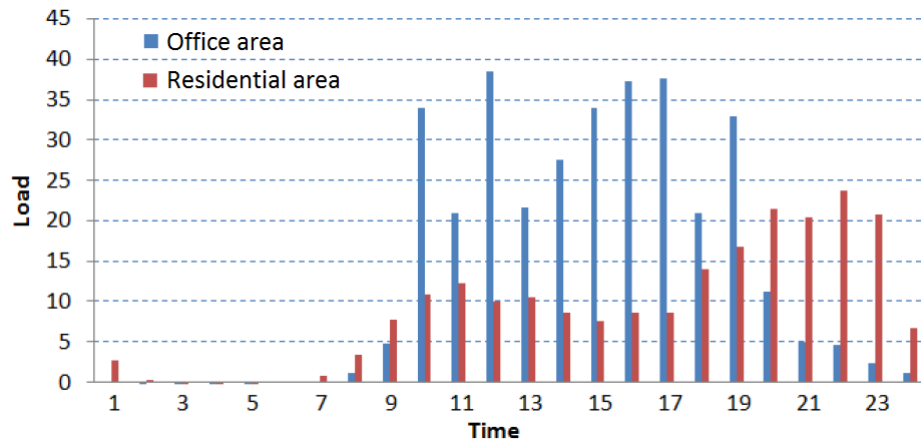


Figure 3.8: Mobile Network Load in Daytime

Thus, during the day, BSs in business areas are oversubscribed and the ones in residential areas stay idle, wasting a large amount of power, while nights are characterized by an opposite behavior. The waste is even bigger considering that BSs are dimensioned to handle a peak value of users, so, given an average number of users, even an active BS usually wastes a fraction of its processing capacity. C-RAN architecture is able to overcome this drawback and free up the capacity in order to fully exploit the processing potential of the BSs and cause a boost from the point of view of energy efficiency.

Another benefit is represented by the concept of virtual cell, also known as dynamic cell structuring, able to overcome the problem of limited coverage of the mm-wave smallcell BSs. C-RAN architecture is able to dynamically control smallcells structures in order to track high traffic users, exploiting beamforming techniques. Moreover, the hidden terminal problem introduced by beamforming technology can be avoided, as the C-plane is managed by macro BS in C-RAN architecture. The possibility of tracking users enables the concept of smallcell BS dormancy, as mmwave BSs can be switched on and off according to the users variable locations, enabling the possibility to save power consumption. An improvement in the scalability field is available too, as it's enough to install new RRHs and connect them with the BBU pool to cover a larger area or split the cell in order to obtain higher capacity. The other main advantages achievable from the use of such technology can be summarized as easier installation, higher performances and improved flexibility [67].

3.5 Initial cell discovery

The possibility to exploit phantom cells and their high capacity is based on the establishment of a UE-smallcell BS connection. The analysis exposed so far shows how mm-wave performances depend on the application of beamforming techniques. For this reason, the exclusive application of highly directional transmissions greatly complicates initial cell search, as both BSs and MSs are required to scan over several directions before synchronization signals can be detected. As a result of directional transmitting and listening, the signal strength is strongly dependent on the propagation directions chosen by the configurations of both antennas, making more difficult to perform carrier sense successfully. This is the reason of the so-called *deafness problem* [68], that arises when a transmitter fails to communicate to its expected receiver because the latter is beamformed toward a direction away from the first. Figure 3.9 shows a graphical representation of deafness problem:

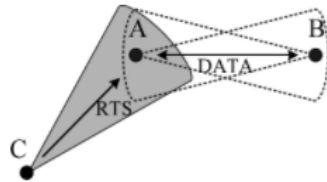


Figure 3.9: Deafness problem

Nodes C and B are respectively the transmitter and the receiver, and the route from C to B passes through node A. When A obtains a data frame from C, it beamforms towards B and forwards the frame accordingly. Node C is unaware of the transmission between A and B, since it cannot receive the directional RTS frame sent from node A to node B. If C starts the next transmission with a RTS frame to A, it will not receive the CTS reply from A, since A is beamformed to B and it cannot receive the RTS frame. Node C retransmits the RTS when A does not respond, and this introduces delay due to the back-off mechanism. This process will go on until the RTS retransmitting limit has been reached, and this will cause a waste of the network capacity.

Antenna directivity is extremely convenient for data communication once MS-BS connection is established, however this last procedure introduces nontrivial challenges. First of all, the link establishment requires that the MS detects the BS: this scanning procedure may delay BS detection and can be very problematic, especially dealing with handover [69]. Then, after the procedure succeeds and the MS has detected a BS, detection of initial random access signals from the MS may be delayed since the BS is required to be aligned in the correct direction.

Current cellular systems have substantial support for beamforming and multi-antenna technologies: for example, 3GPP LTE exploits beamforming technique in order to improve transmission to users at the cell edges, while MIMO technology increases data transmission robustness and data rates, respectively exploiting transmit diversity and spatial multiplexing [70]. However,

the underlying model envisages that initial cell discovery can be completely conducted by exploiting omnidirectional transmissions. For example, LTE BSs generally do not apply beamforming when transmitting the PSS (Primary Synchronization Signal), SSS (Secondary Synchronization Signal) and broadcast signals [71]. The BS sends periodically synchronization signals, the MSs scan the channel with the aim of detecting the BS and starting the synchronization procedure. So, directional transmissions, exploiting adaptive beamforming techniques, are generally performed only after the physical-layer access has been established [72].

However, dealing with mm-wave transmissions, it may be essential to exploit antenna gain even during the cell search procedure. For this reason, smallcell discovery can be supported by information about the MS location that the macro cell BS provides to the phantom cell BS through C-plane communications. The relevance of the use of such information is emphasized by the disparity between the range at which a BS can be detected, using omnidirectional antennas and therefore neglecting the advantages of beamforming antenna gain, and the maximum range at which high data rates can be achieved, exploiting beamforming techniques, that arises from the availability of high gain mm-wave antennas. Figure 3.10 shows this difference between the two zones, depicted respectively as the green and the gray areas:

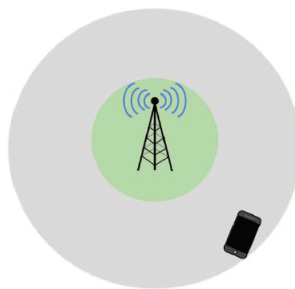


Figure 3.10: Omnidirectional vs directional antennas coverage

This disparity would then create a large area where a MS may potentially be able to obtain a high data rate, but cannot exploiting this possibility because it's unable to detect the BS. If cell search does not exploit this antenna gain, MSs in the gray area may be potentially capable of high data rates, but unfortunately they are not able to locate the base station to establish the communication. This mismatch has gained a major importance dealing with mm-waves: in the low frequency bands, the link budget is sufficiently high and the system works in an interference-limited region, so the difference between the discoverable area and the actual supportable area is minimal. Conversely, for networks exploiting mm-wave bands, the use of the same cell discovery technique will result in a discoverable area that would be much smaller than the actual supportable area, due to the high pathloss at the mm-wave frequency bands.

ALGORITHMS AND LEARNING MEMORY PROCEDURE

This chapter deals with the algorithms that are used to define the sequence of the antenna configurations: Chapter 4.1 is an introduction to the directional cell discovery, while Chapters 4.2, 4.3 and 4.4 are respectively dedicated to a detailed description of random, DGS and EDP algorithms. Chapter 4.5 is used to define the learning memory procedure, while Chapter 4.6 deals with an introduction to localization techniques.

4.1 Directional cell discovery

We described above that the power loss due to the propagation distance, which makes omnidirectional transmissions at mm-wave frequencies unfeasible for typical BS-MS distances in cellular networks, can be compensated for by using highly directional antennas. Moreover, we showed the big mismatch, coming from the use of omnidirectional cell discovery in mm-wave systems, between the small area where a MS can discover a mm-wave BS and the larger one where it can serve a MS exploiting directional antennas. Consequently, the cell discovery process requires the use of directional transmissions in order to fully cover a typical propagation scenario. In order to simplify the discovery procedure, we suppose that MSs and BS are respectively equipped with omnidirectional and directional antennas. Even if a simplified scenario is considered, the main features and mechanisms of the directional cell discovery can be gathered anyway. If conversely we assume that even the MSs use highly directional antennas, the procedure will become more difficult, as it will require that both MS and BS antennas are pointed towards the same direction, in order to avoid the deafness problem described earlier. This solution would clearly result in better performances, as it takes into account receiver gain too, however it may increase dramatically the delay. In this initial work we decided to neglect this possibility and focus to a more general situation, allowing the possibility to analyze this more challenging scenario in future works.

If a BS is able to exploit the information coming from the localization service, sent from MSs to the network exploiting macro cell communications based on U/C-plane splitting, and consequently to determine the position of a MS, beamforming techniques can be applied successfully in order to focus the energy and overcome the mm-wave propagation drawbacks described earlier. The BS calculates a proper antenna configuration, with beamwidth θ_i and pointing direction ρ_i , according to the MS location and consequently beamforwards towards the corresponding direction, in order to perform the tracking and tracing procedures needed for the association phase with the MS. Two main factors, that can dramatically modify the outcome of the connection establishment, can be identified: the presence of obstacles and an imperfect localization mechanism.

We described in Chapter 3.2 that, dealing with mm-wave communications, obstacles have a remarkable impact on propagation mechanisms, acting as opaque elements and obstructing LOS transmissions. As far as localization mechanism is concerned, if the beam is sent towards a direction that doesn't allow reaching the MS, a delay arises due to the time spent to find a proper beamwidth-direction pair. In an ideal scenario, in which there are no obstacles and the BS has perfect information about the propagation environment and MSs location, a suitable configuration will be immediately found and consequently the BS can directly point the MS with a proper beam in a single step.

However, outcomes can be dramatically different if we take into account a more realistic scenario, in which the presence of some obstacles is considered and there is some kind of uncertainty about the MSs location, due to the inaccuracy of the localization service. Moreover, the channel state information may be inaccurate due to the latency needed in obtaining and transmitting them [73]. In such scenario it would be less likely for the BS to reach a MS by using only a single configuration, but conversely it will require a larger amount, due to the unsuccessful switches, even if some techniques based on memory, such as the learning memory procedure that will be described in Chapter 4.5, can be used in order to reduce the number of switches.

Cell discovery could be performed by analyzing all possible antenna configurations until BS and MS point each other. This is not the best available solution, due to the many different antenna configurations available that might delay the whole discovery process. The possibility of using multiple configurations emphasizes the trade-off between the propagation distance reachable by a beam and the area covered: a narrow beam can be used to reach a target very far from the source, by using proper antenna configurations in both transmitter and receiver in order to focus the energy in a very specific direction. On the opposite, a wider beam can propagate its energy covering a larger area, but nearby the transmitter. As a consequence of the different behavior of the beams, a trade-off between the time spent in the process and the range of the environment exploration arises. The use of narrow beams results in greater distances covered by a larger number of beams, since the energy is focused in a more strict way and consequently more beams are needed to cover the whole scenario, and a significant delay due to the amount of configurations to be considered may arise.

The choice of a proper configuration pattern is fundamental for an efficient process, in order to avoid to waste energy and introduce delay during the search of the MSs, because the time spent during the cell search procedure depends on the number of antenna configuration switches needed for the BS-MS link establishment. Performances are influenced by the way in which the sequence of the different antenna configurations to be used is defined: a MS can either be reached by a narrow beam, in order to obtain a higher receiver power and reach longer distances relying on the accuracy of the localization service, or by a larger beamwidth, in order to get a lower received power with a more robust transmission to MS location uncertainty. Three different algorithms taken from [74] have been considered for a simulation campaign and will be described in details in the following sections.

Despite the use of a remarkable set of configurations, however it may happen that none of such configurations is able to reach a MS. Distances may be too large, and the attenuation due to the presence of obstacles implies that the received power may be too low to establish a connection with the BS. Such situations lead to a non-reachability condition, that depends on the MSs and BSs location and the propagation environment, while it is independent on the algorithm used.

4.2 Random discovery algorithm

The easiest way to choose configurations is to pick them in a random way. The first configuration is chosen randomly among all the available ones: if the corresponding transmission is not successful, another configuration is chosen randomly among the set of the remaining ones, with the constraint that every pair of parameters (θ_i, ρ_i) can be chosen only once, until a suitable configuration is found, otherwise the MS is considered as unreachable. Obviously, the main advantage of this algorithm is its easy application, as no information about MS location, antennas or propagation environment is needed and therefore can easily be applied to every propagation scenario. Conversely, no great performances are expected for this algorithm, since no particular criteria are used to choose the configuration sequence. Random algorithm is therefore mainly used as a benchmark to compare performances of more sophisticated algorithms.

4.3 DGS algorithm

An improvement with respect to the random procedure is represented by the choice of a greedy approach, in particular by exploiting the so-called Discovery Greedy Search (DGS) algorithm. The logic behind DGS is to start the discovery procedure exploiting an initial configuration with beamwidth θ based on the environment information: if the MS is not detected, the algorithm chooses the following configuration in clockwise direction with the same beamwidth θ and repeats this operation until all the configurations with a beamwidth equal to θ have been tested, namely all possible directions are considered, and resulted in no successful discovery. If all the configurations analyzed are not able to find the MS, then the algorithm chooses the beam with

beamwidth $\theta_1 < \theta$ that propagates in the same direction of the initial beam, and after tries all possible configurations with beamwidth θ_1 in clockwise direction. The beamwidth narrowing allows propagating the energy with a more strict beam and covering greater distances, so the use of a narrower beam allows reaching farther MSs. Figure 4.1 shows a representation of how the algorithm works, starting from the estimated MS location (x_0, y_0) :

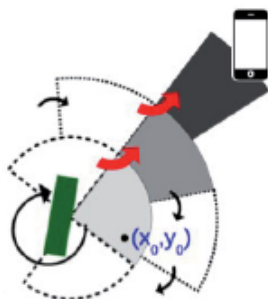


Figure 4.1: Discovery Greedy Search

The algorithm repeats the reduction process until the MS is detected. If all the available configurations are considered and result in no success, the MS is considered as unreachable.

4.4 EDP algorithm

The last algorithm considered in this work is called *Enhanced Discovery Procedure* (EDP). The logic behind EDP algorithm is that, when the localization service suggests the coordinates of the location of a MS, and these coordinates are not absolutely correct, it may be useful to search the MS also nearby the estimated location. Instead of focusing first on all the configurations with the same beamwidth as in DGS, by using an approach that includes also the ones that propagate in completely different directions with respect to the configuration that has just unsuccessfully tested, the approach used in EDP algorithm first takes into consideration an initial configuration based on the environment information, subsequently the ones that propagate with a direction similar to the ones previously used.

The propagation environment can be considered as uniformly divided in sectors, based on the MS estimated location. If the initial configuration cannot detect the UE, then the algorithm explores all the configurations that propagate in the same sector of the first configuration, starting from the ones that have the same beamwidth, alternating clockwise and counter-clockwise directions symmetrically with respect to the first configuration of the sector, and then reducing the beamwidth. If no successful configurations are found in the first sector, then the procedure is repeated also in the second sector, centered in a configuration obtained by a clockwise rotation of $\frac{2\pi}{n}$ rad, where n is the number of sectors considered, and eventually also in the others, with a $\frac{2\pi}{n}$ rad clockwise and counter-clockwise alternate rotation. Figure 4.2 shows the sector division

based on the MS estimated position and the configuration sequence in a single sector:

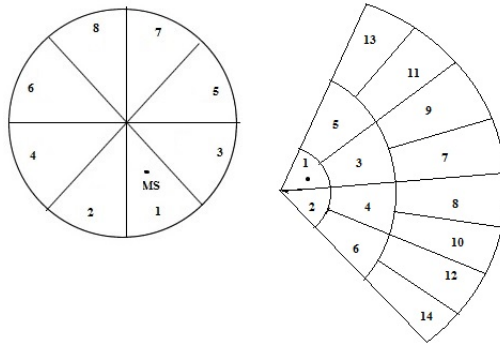


Figure 4.2: Enhanced Discovery Procedure

EDP ends when a successful configuration is found, just as it happens dealing with all the other algorithms, or all the sectors have been unsuccessfully analyzed.

4.5 Learning memory mechanism

So far, independently from the algorithm used, each BS-MS connection is considered individually, without taking into account the previous connections, especially neglecting the information they can offer. However, in a real simulation campaign, it's reasonable to suppose that, as the number of connections increases, a better description of the propagation environment can be obtained, leading to the idea to introduce a mechanism that takes into consideration the results of the previous simulations, and the so-called *learning memory* can help in achieving this goal.

When the presence of obstacles and the MS location inaccuracy prevent establishing the BS-MS connection by using a single configuration, learning memory mechanism can produce an improvement of the discovery delay: the BS can use the configuration evaluated from the channel estimation as a starting point, or can decide to begin the discovery procedure by using the same configuration previously used to reach another MS. When a new MS has to be reached, the memory should be used to find a configuration used previously for another MS that can work with the new one too. The rationale behind the concept of learning memory is that, if a configuration is suitable also for the new MS and it results in a successful transmission, a reduction of the delay in the search procedure can be obtained, as the BS immediately finds the MS. If the previous configuration results in an unsuccessful propagation, then the search for the MS will continue according to the sequence given by the features of the specific algorithm used in the procedure. A basic mechanism considers a local database that stores the information location and the antenna configuration successfully used for each previous MS, even if more sophisticated techniques allow improving the quality of the stored information, by adding for example channel gain predictions or MS spatial distribution [75].

Even if the memory effectiveness is partially influenced by the randomness of radio elements and obstacle locations of each specific propagation environment, however the memory range and the amount of data stored in memory have a not negligible impact on the final results. A memory range is used to filter the stored data: when a BS gets the location information about a new MS, it analyzes the configurations previously used for the MSs that are positioned in a circular area centered in the MS estimated location and with radius equal to the memory range. The choice of the proper memory range is a key point for having an effective learning memory procedure, as the larger is the memory range, the higher will be the number of MSs that may successfully or unsuccessfully suggest the starting configuration.

An increase of the number of connections implies that the memory becomes more and more populated, because it is updated every time a new successful connection is established with the configuration and location information about this MS, therefore the number of MSs that are suitable for a new one increases too. The choice of an effective criterion to find the MS, among all the suitable ones, that suggests the initial configuration is fundamental, and different criteria can be applied to meet this requirement. Given the estimated position of the new MS obtained from the localization service, the starting configuration can be the one previously used for the nearest MS, or can be chosen randomly among the k nearest MSs. Moreover, the uncertainty about the MSs location and the potential presence of obstacles should be taken into account, so it's reasonable to identify a proper MS, by using one of the criteria described earlier, but then starting the discovery procedure by using anyway a configuration based on the environment information instead of always exploiting the memory.

Among all the techniques described so far, a detailed description of the mechanism features used in this simulation campaign will be given in Chapter 5.1. The numerical results that will be described in Chapter 5 will show how different levels of location information accuracy and context features influence the performance of the algorithms and the impact of learning memory on final outcomes.

4.6 Getting location information

We described earlier how accurate information about the MSs location are fundamental in order to exploit beamforming techniques and overcome mm-wave propagation drawbacks. The coordinates can be acquired from an external localization service, exploiting different technologies according to the propagation environment features. In an outdoor propagation scenario, GPS (Global Positioning System) localization service can represent a valid solution [76]: both MSs and BS can be provided with GPS receivers, so the BS is able to obtain data about the MSs location, evaluate the distance to the MS and, exploiting the knowledge of the channel model, properly beamform. The advantages coming from the use of such technology are the use of frequencies in the UHF band, that can exploit better propagation conditions with respect to the mm-wave

band, in particular referred to pathloss and obstacles, and a good precision level of the location, as the 2-5 meters accuracy presented in [77]. Furthermore, the combination of GPS systems and ground support systems and multiband operation can offer an accuracy of 1 meter. Conversely, well-known GPS drawbacks, such as errors due to multipath and receiver clock and mostly the modest performances in indoor context, may limit the wide adoption of such technology for every scenario [78].

The latter drawback leads to the necessity to find other solutions dealing with indoor propagation. The combination of WiFi technology and local radio-based technologies, such as ultra-wide band (UWB), Bluetooth, ZigBee and radio frequency identification (RFID), can result in a submeter accuracy [76]. Moreover, the proposal shown in [57] is based on the use of dual connectivity MSs and WiFi technology to obtain location information. The use of 5 GHz WiFi transmission and mm-wave propagation at 60 GHz can exploit the advantages of both technologies, as in the concept of multiband described dealing with HetNet scenario. The proposed beamforming technique considers a learning mechanism based on the use of 5 GHz WiFi fingerprinting to localize mm-wave best sector IDs in an indoor scenario: when a new MS has to be localized, the comparison of its WiFi signal with the pre-stored WiFi fingerprints allows the BS to evaluate the best beam to reach the MS. The fingerprint is based on the Received-Signal-Strength (RSS) of the MS WiFi signal, even if other WiFi fingerprinting techniques, such as Time Difference of Arrival (TDOA), Direction of Arrival (DOA) and Channel State Information (CSI), are suitable [79]. Figure 4.3 shows a representation of the model, that assumes separate deployments for the 5 GHz WiFi APs, instead of dual band APs, where both WiFi and mm-wave APs are connected to a local controller:

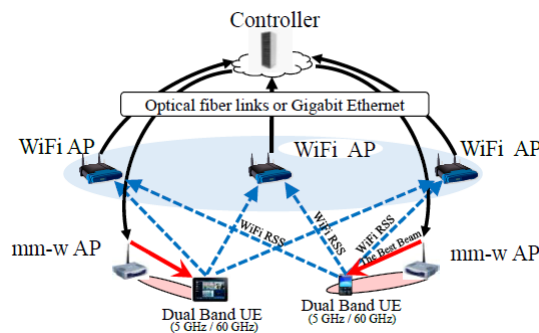


Figure 4.3: WiFi fingerprinting-based localization service

The controller collects the WiFi and mm-wave best sector ID fingerprints, then, after comparing the WiFi readings of the new MS with the pre-stored WiFi samples, it estimates a group of best sector IDs for a mm-wave AP-MS link. Moreover, a beam combining subphase is carried out to find out the best beam with the highest link quality, in order to mitigate the real-time beam blocking and overcome the inaccuracy in WiFi measurements.

NUMERICAL RESULTS

After introducing 5G standard characteristics in the previous Chapters, now numerical simulations, in different propagation scenarios, are considered, in order to better understand the behavior of the three algorithms described in Chapter 4. Chapter 5.1 defines the system model and the propagation environment characteristics, while the following sections are dedicated to a detailed description of the numerical results obtained from the simulations. In Chapter 5.2 an obstacle-free location-error scenario is considered, while Chapter 5.3 considers a scenario with perfect-context information and the presence of obstacles. Chapter 5.4 provides a more realistic representation characterized by obstacles and location information error. Chapter 5.5 consider a scenario in which memory can offer more improved results.

5.1 Propagation model and playground

Numerical results are obtained through a MATLAB simulator, and each presented value is obtained as an average over 100 simulation instances. All antenna gains are modelled as a Gaussian main lobe profile, and a log-distance path loss model is implemented, with a path loss formula considered in this work in the form:

$$PL_{dB} = \alpha + k \cdot 10 \cdot \log_{10} \left(\frac{l}{l_0} \right) \quad (5.1)$$

where $\alpha = 82.02$ dB, the reference distance l_0 is equal to 5 m, l is the distance in meters and $k = 2.36$, for $l \geq 5$ m, while $k = 2$, for $l < 5$ m [17].

For LOS transmissions, the received power formula considered in this work can be expressed as:

$$P_r = \frac{P_t}{PL} \quad (5.2)$$

where the transmitted power P_t is equal to 1 W and PL is the linear form of the path loss value PL_{dB} evaluated from Equation 5.1. A third term G_a is added to the received power formula to account for the antenna gains, therefore received power can be expressed as

$$P_r = \frac{P_t}{PL} \cdot G_a \quad (5.3)$$

where G_a is defined as:

$$G_a = 10^{\frac{G_{a,dB}}{10}}, \quad G_{a,dB} = 10 \cdot \log_{10} \left(\frac{16\pi}{6,76 \cdot \gamma_{ref} \cdot \phi_{ref}} \right) - 12 \left(\frac{\phi}{\phi_{ref}} \right)^2 \quad (5.4)$$

where $\gamma_{ref} = \frac{\pi}{3}$ is the fixed elevation angle, ϕ_{ref} is the beam size and ϕ is the offset between the main lobe beam direction and the azimuth angle.

When transmissions exploit reflection on walls or obstacles, the losses due to the beam impact on reflective surfaces are considered by means of the terms R_{dB} and F_{dB} , defined as:

$$R_{dB} = 20 \cdot \log_{10} \left(\frac{\sin\Theta - \sqrt{B}}{\sin\Theta + \sqrt{B}} \right), \quad F_{dB} = -\frac{80}{\ln(10)} \left(\frac{\pi \cdot \sin\Theta \cdot \sigma}{\lambda} \right)^2, \quad B = \epsilon - \cos^2\Theta \quad (5.5)$$

where Θ , σ and ϵ are respectively defined as the angle of reflection, the roughness and the relative permittivity coefficient of the material. In this simulation campaign, we assume $\sigma = 0.2$ mm, $\epsilon = 4 + 0.2j$ and horizontal polarization [17]. Moreover, the roughness properties of the material, that can bring to a decrease of the power beam, are considered by means of the terms g and ρ_s , defined as:

$$g = \frac{4\pi\sigma \sin(\Theta)}{\lambda}, \quad \rho_s = e^{-\frac{g^2}{2}} \quad (5.6)$$

The surface can be considered smooth for $g < 0.3$. When the surface is rough, the reflected signal has two components: a specular component, coherent to the incident signal, and a diffuse one, which fluctuates in amplitude and phase with a Rayleigh distribution [17]. The specular component reflection coefficient is now equal to:

$$R_{dB} = \rho_s \cdot R_{dB} \quad (5.7)$$

Received power can therefore be evaluated as

$$P_r = \frac{P_t}{PL} \cdot G_a \cdot R \cdot F \quad (5.8)$$

where R and F are respectively the linear forms of R_{dB} and F_{dB} . The minimum received power at the MS necessary to consider the MS as reached by the beam sent by the BS is set to -103 dB.

Cell discovery procedure is performed by exploiting directional transmissions limiting to a 2D plane by using a fixed elevation angle, and considering a division of that plane in three sectors for EDP algorithm. The smallest beamwidth θ considered is equal to 0.0175 rad, allowing to cover the whole propagation scenario by using 360 beams. Larger beamwidths are obtained by reducing proportionally the number of directions to 180; 120; 90; 72; 60; 48; 24; 12; 8; 6; 4; 3; 2; 1, for a total number of 990 available configurations.

The propagation environment is composed of a rectangular deployment area of 450x350 meters, surrounded by four reflecting walls, where 1 mm-wave small cell is placed in the middle and 250 MSs are randomly scattered in the area. The position of the BS is fixed, while obstacles and MSs locations are changed every simulation instance, for a total number of 100 patterns of obstacles and MSs. Different environment schemes are considered, with the deployment of 0, 3, 6 or 9 squared 30x30 meters size obstacles, placed in such a way that they do not overlap, in order to maximize their covered area. Due to the high penetration absorption, we suppose that beams cannot penetrate obstacles and walls, which conversely reflect the incident beams. For the sake of simplicity, the only propagation techniques considered in this work are LOS transmission and through a single reflection on a wall or an obstacle. This assumption allows neglecting transmissions that exploit multiple reflections. Even if MSs are randomly spread in the propagation scenario, however their position is such that a generic MS cannot be completely surrounded by a single obstacle, because, in a 2D propagation, this would surely lead to a non-reachability situation. Conversely, there are no prohibitions in the case of a MS surrounded by more than one obstacle. Figure 5.1 may help to explain these rules:

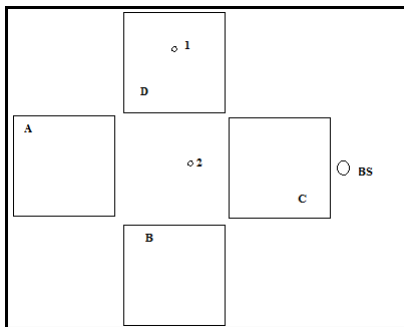


Figure 5.1: Obstacles and MSs location

The example considers a BS, two MSs and four obstacles, indicated respectively as BS, 1, 2, A, B, C and D. Obstacles prevent LOS transmission for both MSs, however MS 1 is surrounded by a single obstacle, namely D, while MS 2 is almost completely surrounded by obstacles A, B, C and D. Due to the fact that MSs are dropped into the environment after that obstacles are placed, all the MSs that would be in a location analogous to MS 1 will be relocated into a new suitable one. All the formulas exposed so far are taken from [17], where further explanations can be found too.

The uncertainty about the MSs location obtained from the localization service is taken into account as a perturbation that is applied to the exact location and that is modeled as a zero-mean Gaussian variable added to its coordinates, leading to a disparity between the MS real location and the position obtained from the localization service. Several values of variance of such variable will be considered, in order to analyze how different degrees of uncertainty impact on final results. As far as the learning memory procedure is concerned, we remind that the BS stores in its local

database the estimated coordinates of the MSs as soon as the discovery procedure succeeds for each single MS, alongside the beamwidth and the direction of the beam used. Among all the available techniques described in details in Chapter 4.5 to manage memory, when a new MS has to be reached, and there is more than a MS in the memory range, the BS always starts the discovery procedure by adopting the same configuration used previously to reach the nearest MS among all the ones that fit in the range.

In order to evaluate the best beam, the BS should have perfect channel information. However, real transmissions are characterized by an uncertainty about such information. For the sake of simplicity, channel path loss and user location errors are considered together through a single equivalent location error. We suppose that the BS is unaware of the position of walls and potential obstacles, therefore its evaluation of the starting configuration according to the channel model will be based only on LOS transmissions. The configuration chosen as the starting point for DGS and EDP algorithm is the one with the largest beamwidth, among all the ones that allow getting a receiver power greater than the threshold by applying Equations 5.2 and 5.3. Although both algorithms use the same starting configuration, their behaviors may be different. Given a generic MS, the BS begins the exploration by using the same configuration, evaluated as if it would exploit a LOS transmission because it has no knowledge about the environment, independently of the algorithm used to define the sequence of the following configurations. If this first transmission is not successful, as there are obstacles in the BS-MS LOS path or the localization service is not accurate enough, then the beamwidth-direction pair of the next beam will depend on the features of the algorithm. The set of available configurations is clearly the same for all the algorithms, but the draft order derives from the features of each of them, so, when the first configuration is not able to reach the MS, the sequence of the following ones will be different. If more than a beam is suitable to establish a connection with the same MS, then it can happen that two databases, used to store data from the use of two different algorithms, will contain two different configurations to reach it. Consequently, when this MS is in the range of a new one and its configuration is chosen as the starting point, it can happen that the configuration descended from an algorithm will result in a successful transmission, while the one obtained from the other algorithm does not work. Algorithms can therefore be compared according to their memory efficacy too: the evaluation of the successful accesses percentage can be used to check whether, for specific propagation conditions, the use of a particular algorithm can offer a more efficient use of memory.

In order to obtain more reliable results, we suppose that the MSs real locations are the same in all the three scenarios, as well as the potential obstacles coordinates. Moreover, the estimated positions depend on the specific location error value, however the application of the same error level would result in the same estimated coordinates in all the scenarios to which it is applied.

5.2 Obstacle-free scenario

In the first scenario, an obstacle-free propagation environment is considered, in which different levels of context information accuracy are compared by means of 6 different numerical values. A Gaussian variable is used to represent the perturbation that implies the inaccuracy of the MS location information, therefore the real MS location is contained with almost absolute certainty in a circular area centered in the estimated position coordinates and with radius equal to the indicated accuracy value.

We begin our analysis by focusing on transmissions without exploiting memory. Figure 5.2 shows the variation of the average number of switches needed for a BS-MS connection according to different accuracy values with the use of DGS and EDP algorithm:

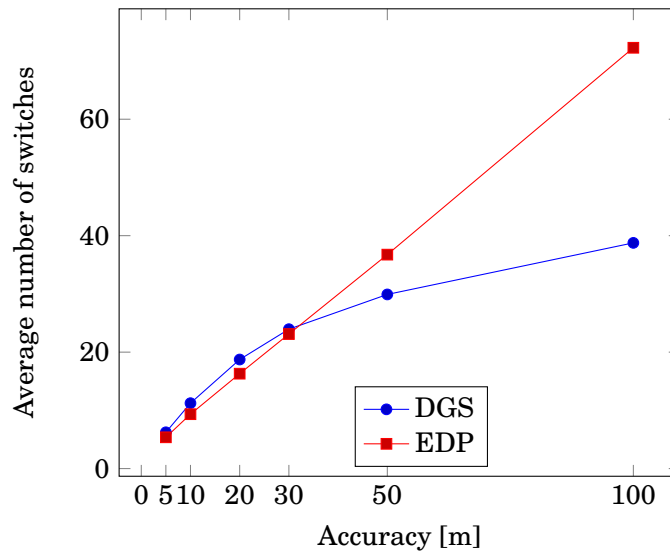


Figure 5.2: Comparison between DGS and EDP in a memoryless scenario

It can easily be observed that both algorithms are characterized by an increase of the average number of switches as a consequence of larger location error values. In an obstacle-free environment with perfect context information, the BS is always able to identify a proper configuration to establish immediately the connection with a MS. When location errors imply uncertainties about the MS location, the BS might use configurations that are not suitable to establish the desired connection, leading to an increase of the total needed amount.

With low location error levels, the algorithms are characterized by a similar behavior, even if EDP uses on average a lower amount of switches. An analysis of their features shows that EDP is advantaged when the MS real location and the estimated position are in the same sector, while DGS can find more easily MSs that can be reached with few propagations in clockwise direction with respect to the estimated location, while it's remarkably disadvantaged when the BS has to

perform a complete rotation of the plane until it can find a proper configuration. The distance between the real and the estimated location is small, accordingly there is a low probability that the two locations belong to two different sectors. Moreover, in environments with low location errors, it's more likely that the first configuration tested can work even if MS estimated position and real location don't correspond, especially with the use of beams with larger beamwidth. No remarkable drawbacks can be identified by the specific use of an algorithm, therefore only a slight difference can be noticed in the average number of switches between the two algorithms, as shown in details in Tables A.1 and A.2 in Appendix A.

The outcomes change dramatically when a very low accurate localization service is considered, that introduces an outstanding uncertainty about the MSs location. So far, performances of the two algorithms were comparable, conversely now DGS algorithm allows using a much less amount of switches with respect to EDP. The EDP sector division is based on the MS estimated location, so an inaccurate division of the plane is performed when it is far from the real position. This algorithm is disadvantaged if the MS cannot be reached by using any of the configurations that propagate in the first sector, because a remarkable number of unsuccessful switches will be wasted, especially when the MS can be only reached by configurations of the last sector. If the localization service doesn't allow obtaining accurate information, the probability to have a situation like the one just described is not negligible, so the considerable amount of wasted switches will affect the final result significantly. Conversely, DGS is less affected by this kind of situation, as it doesn't take into account the environment sector division and it can offer a better outcome, because negative performances occur mainly when the BS has to cover the whole plane before reaching the MS. This behavior can be highlighted also by observing that EDP has a higher standard deviation of the average number of switches with respect to DGS for every accuracy value. Figure 5.3 shows how EDP final results are deeply affected by the low number of switches for the MS in the first sector and the remarkable amount needed for the MS in the others.

As a consequence of the exploitation of the learning memory procedure described earlier, both algorithms can take advantage of the previous simulations, as shown in Figures 5.4. The behavior of the algorithms resemble the memoryless outcomes, however, with a 30 m accuracy, the use of memory can have a more relevant impact on the final results as it allows DGS to be more convenient than EDP in terms of number of switches, while the memoryless scenario is characterized by an opposite performance.

For all the accuracy values considered so far, the possibility to store information about previous MSs can always lead to an improvement of the number of switches. However, the choice of a proper memory range size is fundamental, as same values can even lead to a worsening of the results. This peculiarity leads to the necessity to find a way to evaluate the optimum memory range size in different propagation conditions, or at least to derive some kind of relationship between memory range and accuracy value.

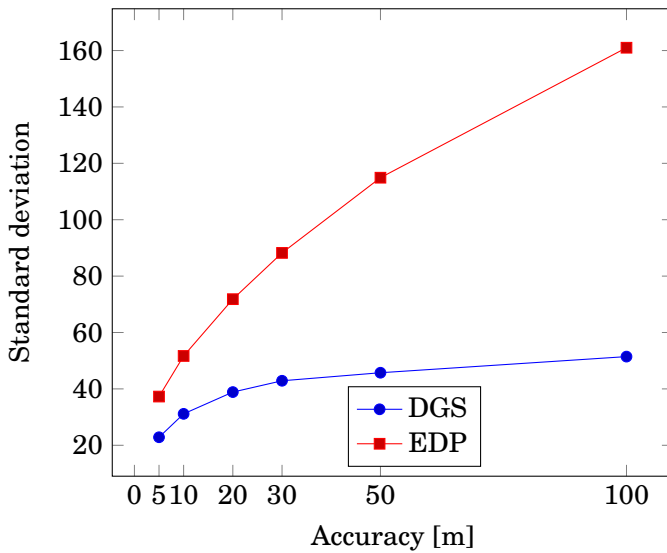


Figure 5.3: Comparison between standard deviation values of the number of switches with DGS and EDP in a memoryless scenario

When two or more past MS accesses are located in the memory range of a new MS estimated position, the first configuration to be tested is always the one used to reach the nearest among them. The comparison between two different memory range sizes implies that the difference of the number of switches derives only from the MSs that are in the bigger range and not in the smaller one. The optimum range is consequently the one that is large enough to include a certain number of MSs and exploit their information, but not so extended to include MSs that cannot be useful. From Figure 5.4 we can observe that each location error value is characterized by a decrease of the number of switches as the memory range increases, until the optimum size is reached, after which any further extension will result in a consequent increase of the number of switches, due to the unsuccessful use of the configurations stored in memory.

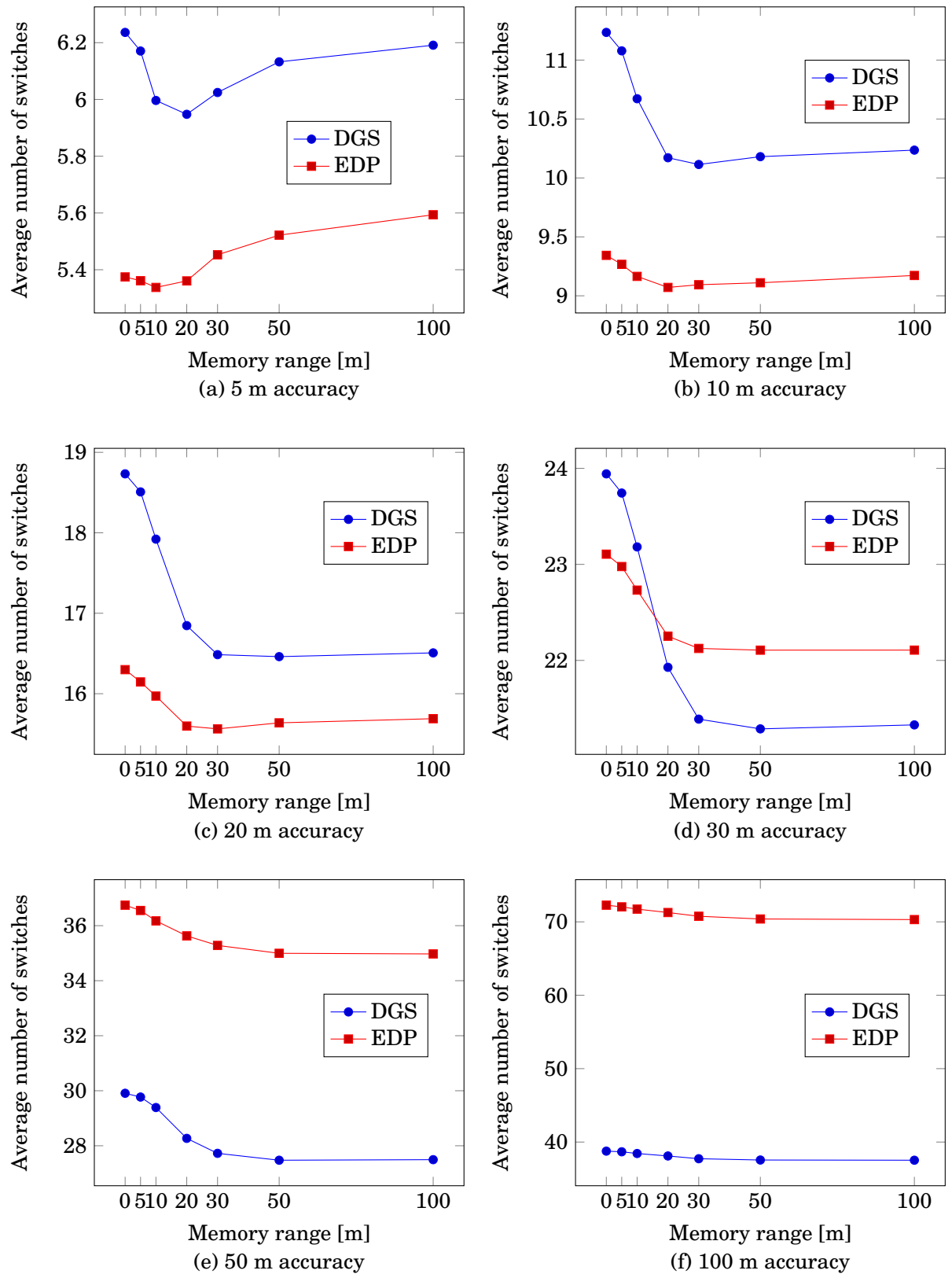


Figure 5.4: Average number of switches for a BS-MS connection in an obstacle-free propagation scenario

For both algorithms we can infer that the optimum range size becomes larger as the location error value increases. In a perfectly accurate environment, the optimum memory size is equal to zero, as the BS can always immediately find a proper configuration and the successful exploitation of the information stored in memory would lead to the use of the same amount of switches. The analysis of environments characterized by location errors is based on how a single memory access affects the total amount of switches. When the configuration stored in memory can be successfully used for a new MS, the connection with that MS will require a single switch, while, without the use of such information, that link would need an amount of switches at least equal to one. Conversely, in case of unsuccessful accesses, the total number of switches needed is the same that can be obtained from the memoryless procedure, with the addition of the configuration stored in memory. The impact of an unsuccessful access is related to the number of switches in the memoryless case. If the BS-MS connection can be realized with a low number of switches as with transmissions in highly accurate environments, then the impact is much greater with respect to communications with high location errors. From the mathematical point of view, if a BS-MS connection requires N switches, an unsuccessful memory access would lead to a total of $N + 1$ switches and consequently to a percentage increase of $\frac{100}{N}\%$. Moreover, a focusing on the amount of switches that can be saved by using memory shows that a successful access reduces the number of switches necessary for that connection from N to 1, with a percentage decrease of $100\left(\frac{N-1}{N}\right)\%$, so the improvement will be as substantial as N is high. Transmissions with high location errors require a higher amount of switches as in Figure 5.2, therefore the decrease will be more emphasized. However, the use of a large memory range would imply that a larger number of far MSs will be used to obtain both successful and unsuccessful starting configurations. Tables 5.1 and 5.2 show the number of saved switches for each memory access, regardless of the positive or negative outcome:

Memory range [m] \ Accuracy [m]	5	10	20	30	50	100
5	1.12	1.15	0.52	0.28	0.11	0.05
10	2.67	2.73	1.92	1.47	1.16	1.03
20	3.70	3.87	3.41	2.95	2.51	2.29
30	3.35	3.72	3.67	3.35	2.94	2.69
50	2.36	2.49	2.97	2.87	2.69	2.48
100	1.53	1.61	1.21	1.36	1.33	1.27

Table 5.1: Saved switches for each memory access with DGS algorithm

Memory range [m] \ Accuracy [m]	5	10	20	30	50	100
5	0.23	0.18	0.03	-0.10	-0.16	-0.23
10	1.30	0.86	0.49	0.33	0.26	0.18
20	2.52	1.57	1.27	0.97	0.73	0.63
30	2.16	1.83	1.56	1.29	1.11	1.03
50	3.31	2.74	2.02	1.93	1.93	1.82
100	3.96	2.67	1.83	1.98	2.07	2.02

Table 5.2: Saved switches for each memory access with EDP algorithm

Low location error values lead to a low optimum memory range size, as, for both algorithms, the improvement obtained from a single memory access using a short memory range is much greater with respect to larger memory sizes, but the considerable increase of the amount of memory accesses due to more extended memory ranges is not large enough to compensate for this difference. Conversely, transmissions with high location errors are characterized by a completely opposite outcome, as the optimum memory range is greater than the one with low location errors. The number of switches that can be saved in a single access by using a low memory range is comparable, and even lower when DGS algorithm is exploited, with the one in the cases of larger memory ranges, which obviously are characterized by a much greater amount of accesses. Analogous outcomes can be found focusing on the number of saved switches for each successful memory access.

In addition to the numerical values just exposed related to the amount of saved switches, the comparison of the percentage decreases can be useful to highlight the behavior of the memory, as shown in Tables 5.3 and 5.4:

Memory range [m] \ Accuracy [m]	5	10	20	30	50	100
5	1.05%	3.85%	4.63%	3.39%	1.66%	0.72%
10	1.39%	5.01%	9.46%	9.97%	9.38%	8.89%
20	1.20%	4.33%	10.07%	12.00%	12.13%	11.88%
30	0.84%	3.18%	8.41%	10.67%	11.09%	10.92%
50	0.46%	1.73%	5.48%	7.30%	8.14%	8.07%
100	0.23%	0.84%	1.70%	2.67%	3.12%	3.19%

Table 5.3: Percentage decrease by learning memory application using DGS algorithm

Accuracy [m] \ Memory range [m]	5	10	20	30	50	100
5	0.25%	0.69%	0.26%	-1.45%	-2.74%	-4.07%
10	0.82%	1.91%	2.91%	2.67%	2.49%	1.83%
20	0.94%	2.02%	4.30%	4.52%	4.06%	3.74%
30	0.56%	1.62%	3.70%	4.25%	4.33%	4.32%
50	0.52%	1.55%	3.04%	3.98%	4.76%	4.82%
100	0.32%	0.74%	1.38%	2.09%	2.60%	2.71%

Table 5.4: Percentage decrease by learning memory application using EDP algorithm

The results show a not negligible impact of the memory, especially dealing with DGS algorithm, that is able to offer a higher percentage improvement with respect to EDP for almost all the accuracy value-memory range pairs. As far as transmissions with low location errors are concerned, EDP allows using on average a lower number of switches with respect to DGS, therefore the percentage improvement obtained from successful memory accesses is expected to be lower. Moreover, the average number of switches of EDP is mostly caused by the great difference between the low amount of switches required by the MSs in the first sector and the high amount needed for the MSs in the others, also proved by the higher standard deviation. EDP can therefore save a high amount of switches only when memory is successfully applied to MSs that are not in the first sector, but in highly accurate environments this situation is not very common. Conversely, DGS can offer a more homogeneous outcome in terms of number of switches, therefore a generic successful access has a higher probability to be applied to a MS with a high starting amount of switches. Furthermore, EDP allows saving a larger total amount of switches with respect to DGS only in poor accurate environments, due to the higher probability to successfully apply memory in order to reach in a single step MSs that are in the last sector. Nevertheless, in these cases the use of EDP results in a similar percentage decrease with respect to the performances of DGS, due to the low percentage of successful memory accesses. In all the accuracy-range pairs considered in this scenario, the average number of successful memory accesses of the two algorithms, neglecting some slight differences, can be considered as equal, as shown in Tables A.3 and A.5 in Appendix A. We can conclude that, as far as memory efficiency is concerned, the two algorithms have an analogous behavior and the specific use of one of these will not produce significantly better results. Full numerical values for this scenario can be found in Appendix A.

5.3 Perfect context information scenario

After focusing on an obstacle-free scenario, here the propagation environment is characterized by perfect context information, in which the MSs estimated locations obtained by the localization service are the positions in which effectively the MSs can be found. The arrangement of 3, 6 and 9 obstacles allows evaluating how physical elements in the propagation environment affect the cell discovery procedure and how they can be successfully overcome by the use of DGS and EDP algorithms. Moreover, the averaged value over 100 MSs and obstacles different patterns can represent a reasonable way to moderate the impact of possible particular situations that may alter the general behavior of the algorithms.

In a similar manner to what was done dealing with the obstacle-free scenario, first of all we consider a situation in which memory is not exploited. Figure 5.5 shows the variation of the average number of switches based on the different number of obstacles:

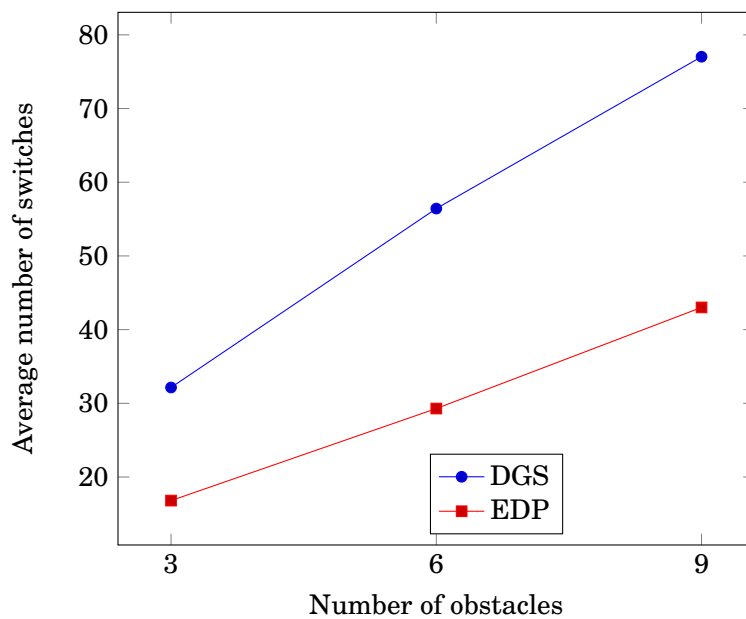


Figure 5.5: Comparison between the average number of switches using DGS and EDP without exploiting memory

From Figure 5.5 it emerges that both algorithms are characterized by an increase of the number of switches as a consequence of the addition of the number of obstacles. In a perfect context information scenario, the presence of obstacles heavily hinders the possibility to establish a BS-MS connection by using only a single configuration due to the assumption that removes the possibility for a beam to penetrate obstacles. The deployment of a greater number of obstacles makes more likely the situation in which an obstacle is located between BS and MS, and consequently increases the average number of switches.

Moreover, for all the three amounts of obstacles taken into account, the use of EDP algorithm

allows on average to obtain a BS-MS connection with a significantly lower number of switches with respect to DGS. When an obstacle prevents the LOS transmission, the BS must rely on configurations that exploit a reflection on a wall or another obstacle. EDP starts the procedure by exploiting configurations that propagate in the sector in which the MS is definitely located, as perfect context information allow knowing the real MS location, focusing the propagation on a more restricted zone and allowing to exploit reflections on walls and obstacles from two directions at a time, due to the alternation between clockwise and counter-clockwise propagation direction. Conversely, DGS algorithm is characterized by an uniform clockwise propagation all over the plane, exploiting even configurations that propagate in completely different directions with respect to the MS location and limiting to a single reflection direction at a time. Two additional unfavorable factors can therefore be identified. The distance covered by the beam increases, and consequently a higher path loss arises. Moreover, the exploitation of beams that propagate further increases the probability to collide adversely with other obstacles or walls, as shown in Figure 5.6:

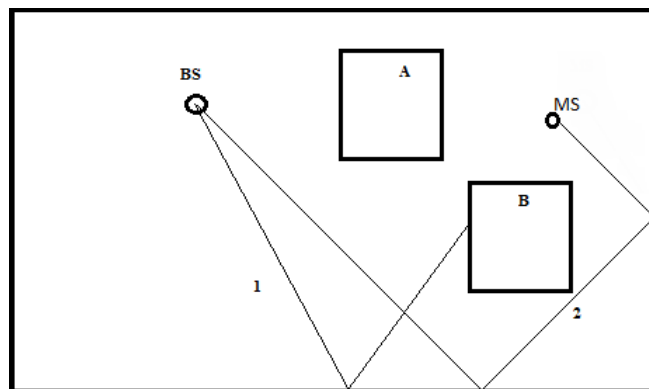
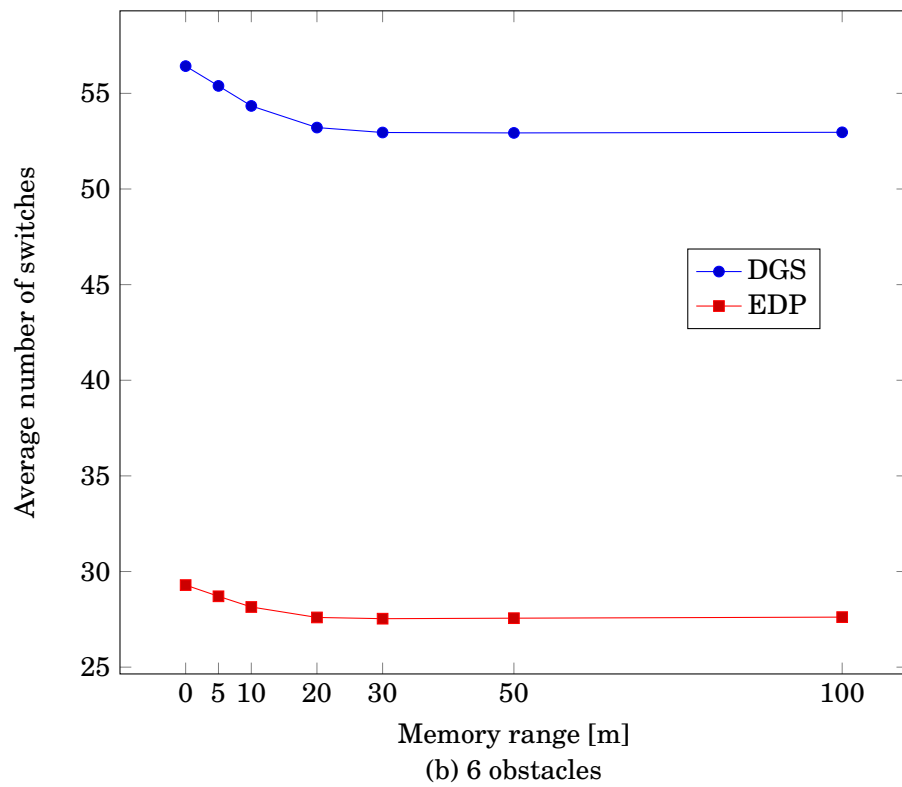
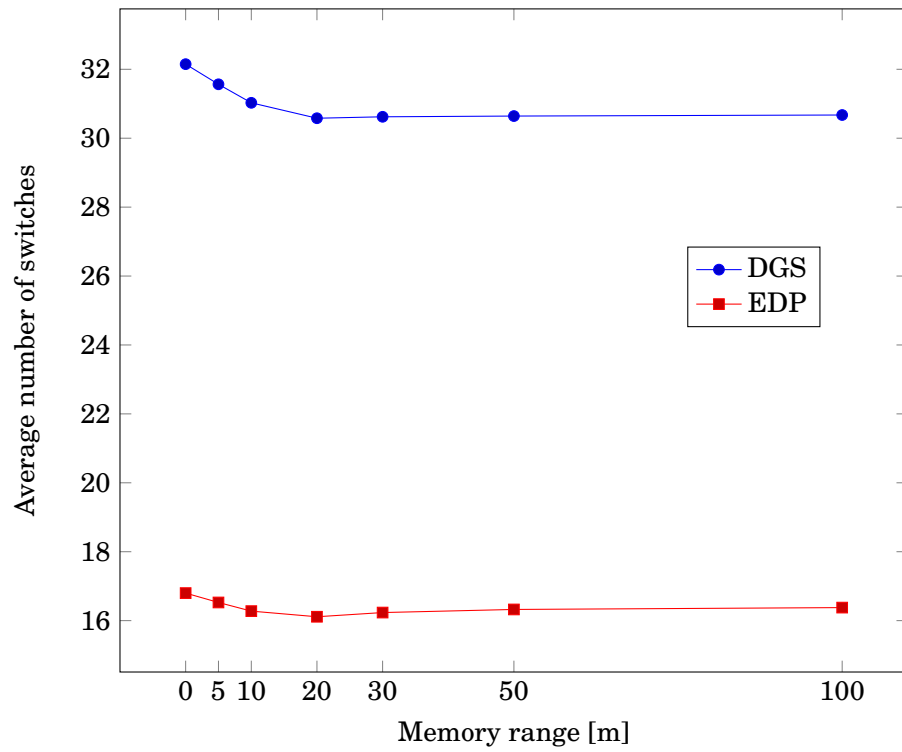


Figure 5.6: Reachability prevented by reflection mechanisms

Obstacle A prevents a BS-MS LOS transmission, so a reflection is required. Beam 1 is reflected by the lower wall and hits obstacle B, while, even if obstacles or walls could be used to exploit multiple reflections, and consequently beams may successfully reach MSs, as happens by using beam 2, however we consider up to a single reflection, so this possibility cannot be contemplated in our analysis.

Figure 5.7 shows the variation of the number of switches when different memory ranges are applied:



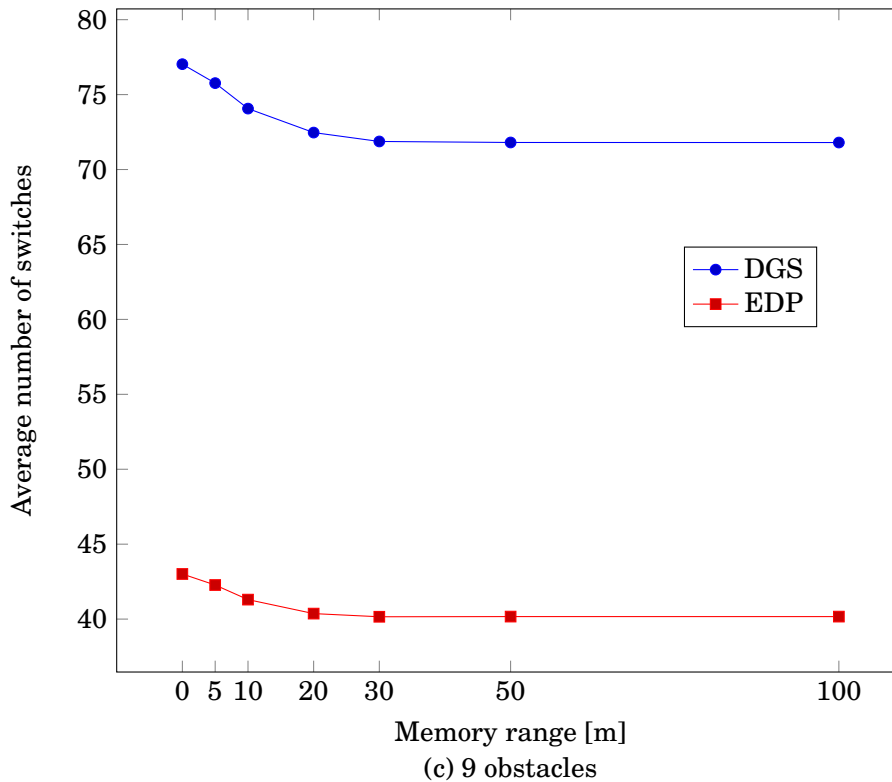


Figure 5.7: Average number of switches when learning memory is applied

We can easily observe that, similarly to what described in the obstacle-free scenario, the number of switches decreases when the memory range increases until we use the optimum range size, then it increases when we consider a larger memory range. The use of a small memory range relies on the assumption that, in the majority of cases, the same configuration can work with two MSs that are physically close, as their propagation conditions can be considered equal, unless an obstacle prevents to reach the second MS by using that configuration. The expansion of the memory range allows considering even more suitable MSs, until we reach the optimum memory range: from now on, any increase of that size will result in an increase of the number of switches, as we unsuccessfully try to use the stored configuration to reach a MS that may be too far from the area covered by that beam or be hidden by an obstacle.

A slightly different behavior can be observed by focusing on the EDP algorithm in the 9-obstacle pattern as in Figure 5.7(c). The optimum range is equal to 30 m, and after that value the number of switches is supposed to continue to increase as the memory range increases. However, Table B.2 in Appendix B shows how the average number of switches with a memory range equal to 50 m is greater than the value obtained with a memory range of 100 m. The reason of such result can be explained starting from Figure 5.8:

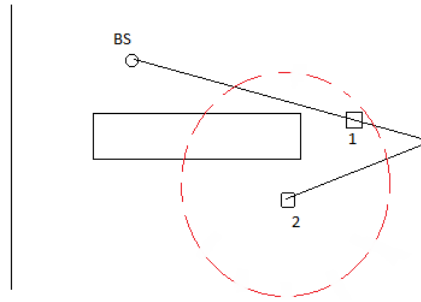


Figure 5.8: Configuration affected by memory range

The propagation environment is composed of a BS, two MS, indicated as 1 and 2, and an obstacle. The configuration used by the BS to establish the connection with MS 1 could successfully be used also to reach MS 2, as MS 1 is in the range of MS 2, depicted as the dashed circle. With a smaller memory range, the BS would not be able to use the information associated with MS 1, and would have to exploit a configuration of the sequence generated by the algorithm. Such situation may actually happen in a real simulation, however it is very uncommon and its impact on the final results is modest. Moreover, its effect cannot be predicted so easily, because the use of that configuration affects also the future simulations, as MS 2 will be stored in memory with the same configuration of MS 1 instead of the one that the algorithm would have suggested.

Both algorithms are characterized by a larger optimum memory range as a consequence of the deployment of a greater amount of obstacles. The knowledge of the MSs exact location in an obstacle-free propagation environment leads to an optimum memory range size equal to zero, namely a memoryless situation, as the BS is always able to evaluate immediately a configuration that, exploiting a LOS transmission, can successfully establish a BS-MS connection. The consequences of the use of memory in that kind of situation are or the successful use of the stored configuration, that however will imply no advantage with respect to a memoryless transmission, or an increase of the number of switches, when the stored configuration is not suitable for the new MS.

The outcomes are completely different when we introduce obstacles in the propagation environment: the remarkable attenuation due to physical elements in mm-wave transmissions brings us to neglect the possibility for a beam to pass through obstacles, so the presence of an obstacle located between BS and MS that impedes LOS transmissions leads to the necessity to use configurations that exploit a reflection to pass around it. The deployment of more obstacles will require a higher number of switches, as in Figure 5.5, therefore the successful exploitation of the memory allows reducing the quantity of switches needed for a BS-MS connection from a higher starting amount to a single switch. The use of a more extended range allows detecting more MSs that could be used to reduce the number of switches, but an improvement arises only when the decrease coming from the successful accesses can completely compensate for the increase due to the unsuccessful accesses.

The evaluation of the average amount of saved switches for every successful memory access, as in Tables 5.5 and 5.6, shows that, for both algorithms, an increase of the memory range corresponds to a decrease of such amount:

Obstacles \ Memory range [m]	5	10	20	30	50	100
	3	11.84	7.62	5.26	4.31	4.01
6	22.75	15.35	11.57	10.59	10.04	9.84
9	29.82	24.11	18.23	17.18	16.31	16.22

Table 5.5: Saved switches for each successful memory access with DGS algorithm

Obstacles \ Memory range [m]	5	10	20	30	50	100
	3	5.52	3.56	2.30	1.60	1.27
6	12.88	8.44	6.10	5.36	4.98	4.77
9	17.47	13.96	10.58	9.53	8.90	8.84

Table 5.6: Saved switches for each successful memory access with EDP algorithm

This outcome can be proved considering, for example, a situation in which a BS uses a short-range and a large-range memory. The use of a large-range memory increases the possibility to face situations in which the BS would be able to establish the connection with a MS by using a single configuration even without the use of memory, but the information stored forces it to access the memory and use the specified configuration. As a consequence, the number of successful accesses increases, while the total number of switches remains the same. The evaluation of the average number of saved switches due to the use of memory shows that short-range memory is characterized by a lower number of accesses and consequently by a higher amount for each access. A similar ending can be found also removing the limitation on the successful outcome of the memory accesses, as now large-range memories increase the possibility to face situations in which the stored configuration is not suitable for the new MS, leading to an increase of the total number of switches and a consequent decrease of the average number of saved switches. Moreover, it can be observed that the arrangement of more obstacles allows saving a larger average amount of

switches with a single access for all the memory ranges considered, that can be easily proved focusing on the higher amount of switches that characterizes those environments.

From the comparison between algorithms, it emerges that the use of DGS always allows saving a considerably larger quantity of switches for every memory access with respect to EDP. The number of total memory accesses is clearly the same for both algorithms, while there is only a slight difference in the successful memory attempts quantity, as shown in Tables B.3 and B.5 in Appendix B, therefore DGS allows saving a total quantity of switches that is consequently larger than the amount which can be obtained by the use of EDP. The reason of this outcome is that DGS algorithm needs on average a larger quantity of switches than EDP, so the successful exploitation of the memory can reduce from a higher quantity of configurations to a single one. However, a comparison of the percentage decreases shows that, especially in environments with a higher number of obstacles, both algorithms can offer similar performances, as in Tables 5.7 and 5.8:

Obstacles \ Memory range [m]	5	10	20	30	50	100
	3	1,82%	3,49%	4,88%	4,75%	4,68%
6	1,84%	3,69%	5,69%	6,15%	6,19%	6,13%
9	1,64%	3,85%	5,93%	6,70%	6,78%	6,79%

Table 5.7: Average percentage decrease with DGS algorithm

Obstacles \ Memory range [m]	5	10	20	30	50	100
	3	1,62%	3,11%	4,09%	3,36%	2,83%
6	2,00%	3,91%	5,78%	6,00%	5,91%	5,72%
9	1,71%	3,98%	6,15%	6,64%	6,61%	6,61%

Table 5.8: Average percentage decrease with EDP algorithm

For this reason, although the remarkable improvement in terms of saved switches, EDP can be used to establish connections by using a lower number of switches with respect to DGS even after the exploitation of memory. Full numerical values for this scenario can be found in Appendix B.

5.4 Realistic scenario

In the last case, a more realistic scenario is considered, in which the presence of 9 obstacles is combined with a variable uncertainty about the MSs location. Performances of both DGS and EDP are compared with the random algorithm, that is used as a benchmark to better analyze the benefits obtained from such improved techniques.

As we did dealing with the other two scenarios, the analysis begins with a comparison of the three algorithms' behaviors in a memoryless situation, as shown in Figure 5.9:

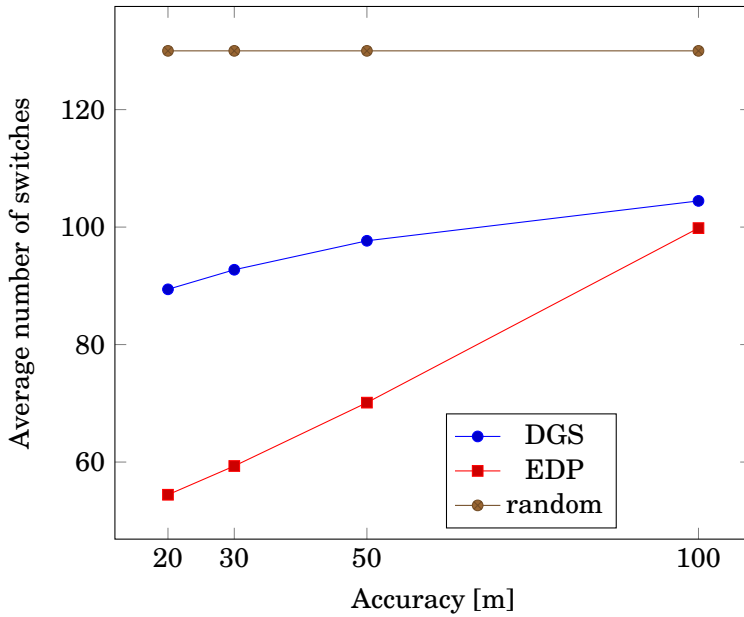


Figure 5.9: Comparison between algorithms in a memoryless 9-obstacle scenario with location errors

Similarly to the outcomes in the obstacle-free scenario, an increase of the location error value implies an increase of the average number of switches when DGS and EDP are applied, due to a greater uncertainty about the MSs location. This trend is not observed by adopting the random algorithm, as it does not consider data coming from the localization service, so a worsening of the accuracy of such information has no impact on the final results. Moreover, the behavior of random algorithm is significantly worse than that of DGS and EDP as regards the average number of switches, due to the benefit obtained by the use of the localization service, which can be further proved by observing that this worsening decreases when less accurate environments are considered.

As far as EDP and DGS are concerned, EDP is characterized by a better behavior in all four location error values considered, due to its ability to identify the sector in which the MS is supposed to be located and propagate accordingly. However, the difference between algorithms decreases as the localization information become less accurate, due to the impact of sector division

of the plane that implies the unsuited propagation features of EDP when the MS is actually in another sector and the consequent greater number of MSs that will experience this condition.

A comparison with the obstacle-free scenario, as shown in Figure 5.10, can be useful to highlight how performances are affected by the deployment of obstacles:

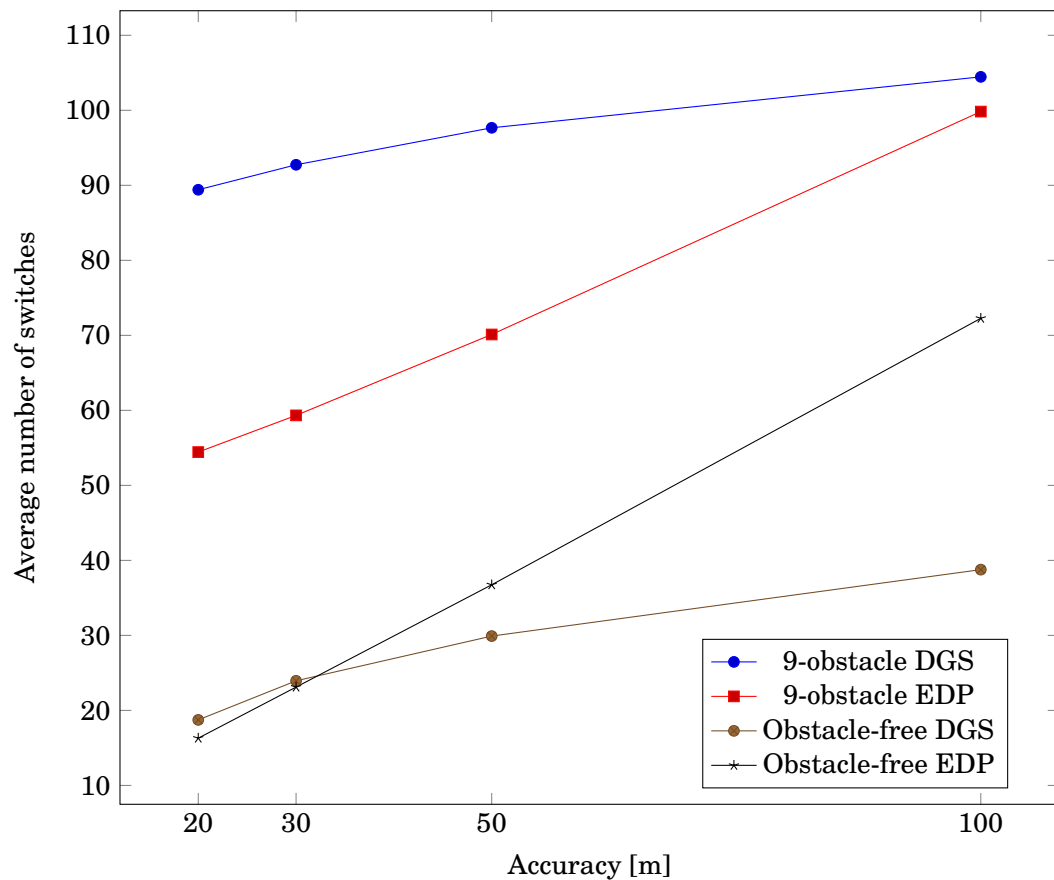
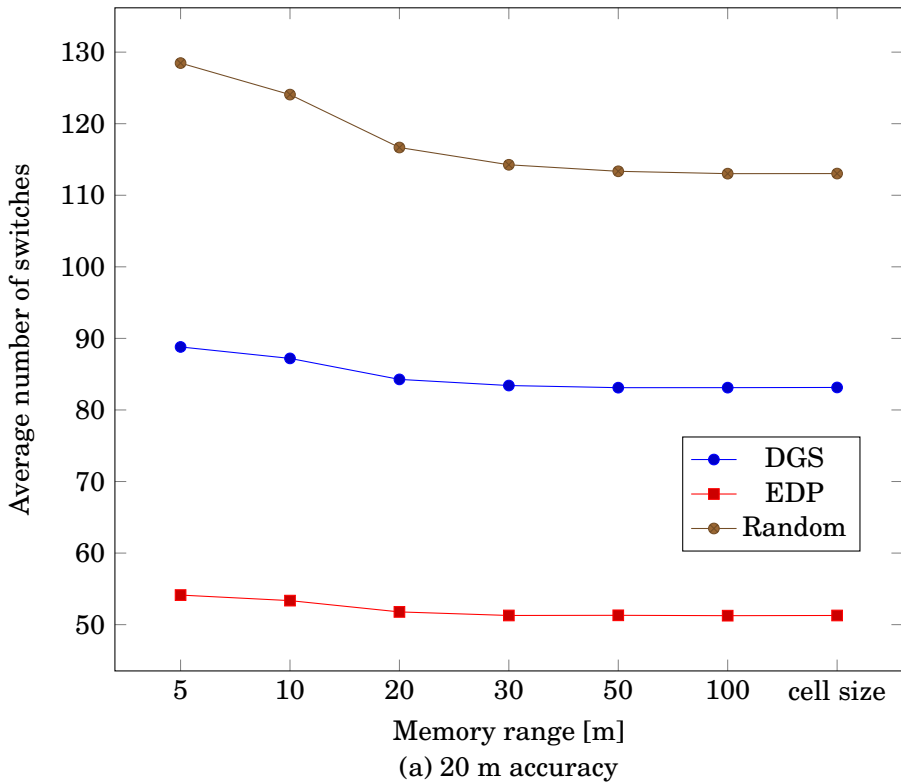


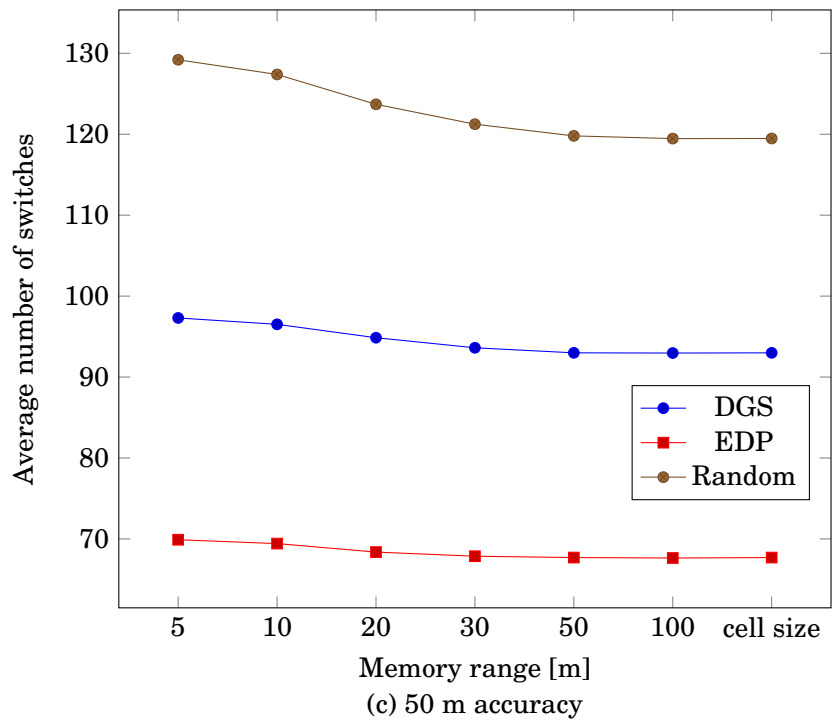
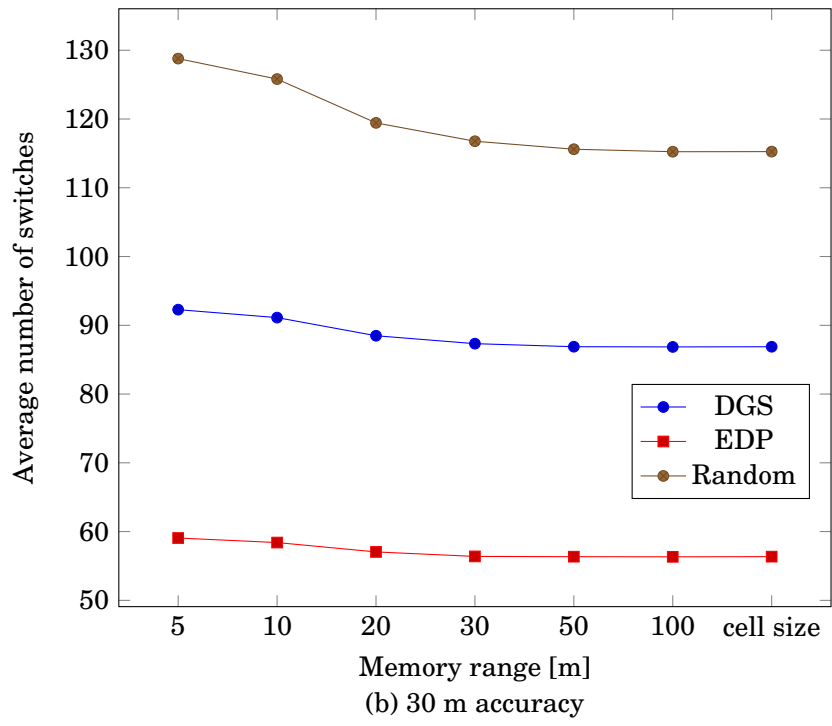
Figure 5.10: Comparison between DGS and EDP in a memoryless obstacle-free and in a memoryless 9-obstacle scenario with location errors

The trends of both algorithms resemble the obstacle-free scenario, however a remarkable difference can be observed by comparing the performances of the two scenarios. While now the use of EDP has a more restricted worsening in terms of number of switches, DGS has a considerably worse behavior with respect to the obstacle-free scenario. As described in Chapter 5.3, DGS features imply a single direction of rotation, therefore an obstacle preventing LOS transmission has a greater impact in terms of wasted switches. Conversely, the uncertainty about the location has a minor impact, because its influence conditions the results in a minor way as shown in Chapter 5.2 and its effect may be partly mitigated by the presence of obstacles covering a large area nearby the MS real location. This difference can be already seen applying a low location error value, to show how performances of DGS are more significantly affected by the presence of obstacles than by the accuracy of the MSs location information.

Conversely, the increase of the location error value does not imply a great increase of the number of switches with DGS, on the contrary of the behavior of EDP. As shown in Chapter 5.2, EDP is strongly influenced by the sector division, and a remarkable increase of the number of switches can be observed when a low accurate localization service implies that, with a higher probability, MS real location and estimated position belong to two different sectors.

After describing memoryless simulations, we take into account the use of the learning memory procedure. To better evaluate the benefit coming from the use of the memory in a real scenario, we consider even a memory range equal to the propagation environment size, so that the BS can always find a MS that provides the initial configuration, if the memory stores information about at least a MS. Figure 5.11 shows the variation of the average number of switches following the application of different memory ranges on propagations characterized by four different accuracy values with the use of DGS, EDP and random algorithms:





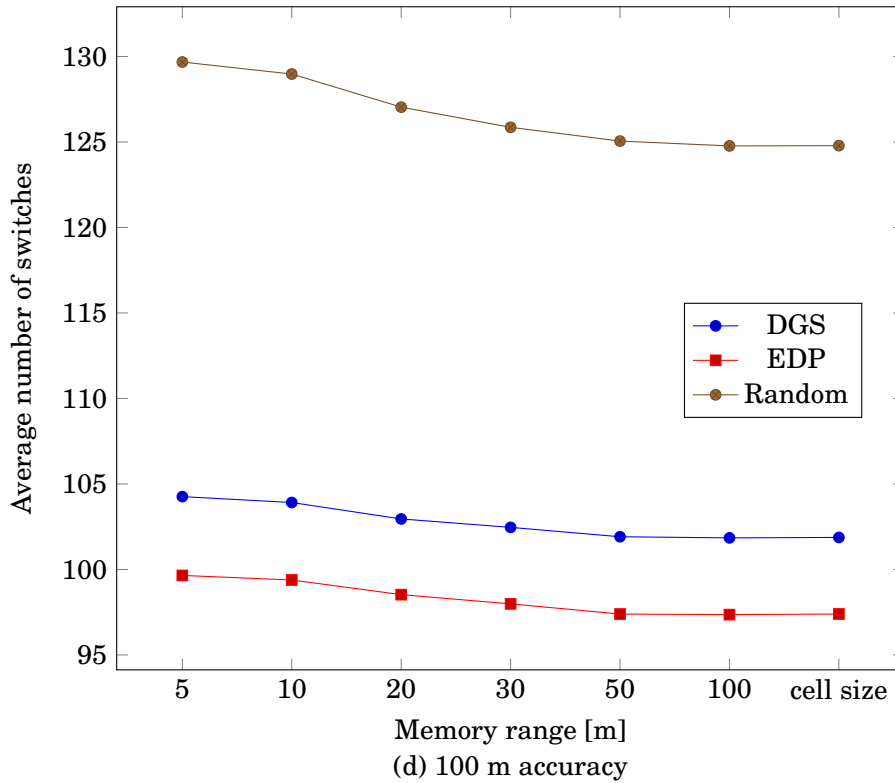


Figure 5.11: Variation of the number of switches when different accuracy values are applied

All the three algorithms are characterized by a high starting value, which decreases as the memory range increases until the optimum range is reached, after which the number of switches increases. We can observe that the optimum range size behavior resembles the obstacle-free scenario, but now it's characterized by a very low increase when we consider less accurate environments. All the algorithms are characterized by a decrease of the total amount of saved switches when a higher location error value is applied, as it limits the efficacy of the memory. Despite an increase of the total amount due to the higher number of successful memory accesses, a detailed analysis shows how an increase of the memory range is associated to a decrease of the average number of saved switches, as in Tables C.7, C.10 and C.13 in Appendix C. The use of larger ranges implies the application of memory even for MSs that could be reached in a single step even without using the stored configuration, in addition to an increase of the number of unsuccessful attempts. The analysis of the successful memory accesses shows that the amount of saved switches is similar in all the memory range sizes considered, as respectively in Tables C.8, C.11 and C.14 in Appendix C. Random algorithm is however characterized by a higher amount of saved switches with respect to the other algorithms, due to the higher number of switches in memoryless transmissions, in addition to an increase of such amount when more accurate environments are considered.

The percentage saves obtained by the use of the memory are shown in Tables 5.9, 5.10 and 5.11:

Obstacles \ Memory range [m]	5	10	20	30	50	100	cell size
20	0,67%	2,46%	5,74%	6,70%	7,04%	7,03%	7,01%
30	0,50%	1,74%	4,59%	5,83%	6,31%	6,34%	6,31%
50	0,38%	1,18%	2,88%	4,15%	4,79%	4,81%	4,79%
100	0,19%	0,52%	1,44%	1,91%	2,44%	2,50%	2,47%

Table 5.9: Percentage decrease using DGS algorithm

Accuracy [m] \ Memory range [m]	5	10	20	30	50	100	cell size
20	0,56%	1,98%	4,88%	5,79%	5,75%	5,84%	5,79%
30	0,45%	1,56%	3,86%	4,95%	5,02%	5,05%	5,01%
50	0,31%	0,99%	2,48%	3,21%	3,45%	3,53%	3,45%
100	0,18%	0,45%	1,30%	1,84%	2,44%	2,47%	2,44%

Table 5.10: Percentage decrease using EDP algorithm

Accuracy [m] \ Memory range [m]	5	10	20	30	50	100	cell size
20	1,18%	4,57%	10,25%	12,11%	12,81%	13,06%	13,05%
30	0,94%	3,23%	8,13%	10,18%	11,07%	11,35%	11,34%
50	0,62%	2,01%	4,85%	6,74%	7,85%	8,11%	8,10%
100	0,25%	0,79%	2,28%	3,19%	3,81%	4,02%	4,01%

Table 5.11: Percentage decrease using random algorithm

These tables show that the use of memory applying DGS and EDP algorithms leads to a similar behavior in terms of percentage decrease of the number of switches, while memory can bring to a considerably better result as far as the use of random algorithm is concerned. Two main reasons are behind this result: first of all, random simulations need on average a much greater quantity of switches with respect to the other algorithms, therefore the successful use of

memory can reduce more dramatically the number of switches. Moreover, DGS and EDP rely on a sequence that is defined after that the MS location is known, therefore memory is applied in a context already improved by the localization service information. Conversely, random algorithm does not exploit the information about the propagation environment, therefore a greater decrease is expected as the exploitation of memory is the only way to improve performances.

Even if the benefit just presented is not negligible, especially dealing with random algorithm, however this very algorithm is extremely inefficient in terms of percentage of successful memory accesses when compared with EDP and DGS. Tables 5.12, 5.13 and 5.14 show the variation of the percentage of successful memory accesses according to the accuracy values and the memory ranges:

Memory range [m] \ Accuracy [m]	5	10	20	30	50	100	cell size
20	56,40%	52,89%	44,78%	39,03%	33,35%	30,30%	29,27%
30	43,59%	43,23%	38,90%	34,59%	29,78%	27,14%	26,27%
50	29,83%	31,07%	28,61%	26,39%	23,68%	21,62%	20,96%
100	14,72%	14,41%	14,12%	13,35%	12,58%	11,88%	11,53%

Table 5.12: Average percentage of successful accesses using DGS algorithm

Memory range [m] \ Accuracy [m]	5	10	20	30	50	100	cell size
20	55,85%	52,77%	44,66%	38,98%	33,33%	30,31%	29,28%
30	43,04%	42,97%	38,78%	34,42%	29,69%	27,03%	26,16%
50	30,06%	30,85%	28,52%	26,25%	23,57%	21,52%	20,87%
100	14,49%	14,59%	13,87%	13,06%	12,42%	11,65%	11,32%

Table 5.13: Average percentage of successful accesses using EDP algorithm

Accuracy [m] \ Memory range [m]	5	10	20	30	50	100	cell size
20	31,83%	31,72%	27,46%	24,04%	20,65%	18,96%	18,34%
30	24,23%	24,24%	22,89%	20,66%	18,04%	16,60%	16,08%
50	16,59%	15,71%	15,13%	14,51%	13,29%	12,36%	12,00%
100	8,36%	7,90%	7,65%	7,44%	7,11%	6,81%	6,62%

Table 5.14: Average percentage of successful accesses using random algorithm

While, for every accuracy value-memory range pair, DGS and EDP percentages can be considered as analogous, as only slightly differences can be observed among the values, random algorithm is characterized by a definitely worse behavior. This outcome can be proved by focusing on the different beam typologies that are exploited by the random algorithm with respect to the ones used by EDP and DGS. An analysis of the data stored in the memory can be useful to better understand this result. For this purpose, a generic simulation, with an accuracy value of 20 m and a memory range of 5 m, is performed, and the playground representation is shown in Figure 5.12:

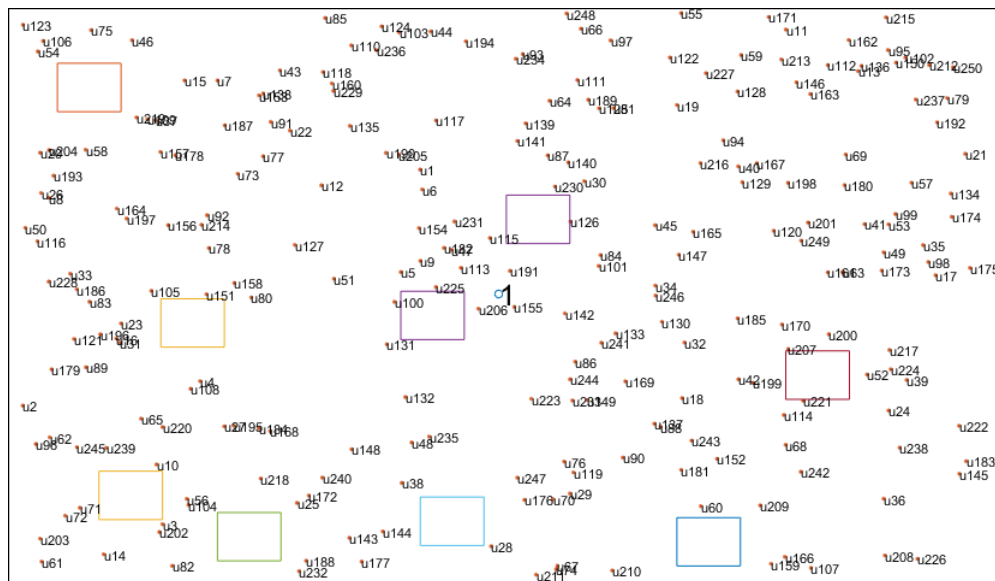


Figure 5.12: Playground representation

Table 5.15 shows the number of beams that exploit each of the three transmission ways considered in this work, namely LOS transmission, reflection on a wall and reflection on an obstacle:

Beam typology Algorithm	LOS transmission	Reflection on a wall	Reflection on an obstacle
DGS	159	31	13
EDP	163	31	9
Random	133	39	31

Table 5.15: Memory content of a generic simulation

We can observe that random algorithm relies to a greater extent on configurations that exploit reflection than the other two algorithms, in particular there is a greater number of MSs whose connection with the BS is based on reflection over an obstacle. Two main factors hinder good performances: the exploitation of reflected beams in a scenario with obstacles increases the probability of an impact with an obstacle when they are used as a starting configuration with another MS. Moreover, the use of reflected beams instead of LOS transmissions requires a greater accuracy of the location information, and the relevance of accurate data can be observed even analyzing the beamwidth of the beams used in the simulation, as shown in Table 5.16, where the number of beams with beamwidth equal to 3° , 2° and 1° is listed:

Beamwidth Algorithm	3°	2°	1°
DGS	10	9	24
EDP	12	7	24
Random	33	36	63

Table 5.16: Number of beams with narrow beamwidths

We can observe that the quantity of beams with narrow beamwidths used by the random algorithm is definitely greater with respect to the DGS and EDP. In particular, random algorithm uses more than double of the thinnest beams than the other two algorithms. The use of narrow beams is particularly disadvantageous in a scenario with location errors, if the new MS and the one that suggests the starting configuration are not too close. There are several MSs for which EDP and DGS prove that a larger beam could be used, however the randomness of the algorithm neglects to fully exploit this possibility. Full numerical values for this scenario can be found in Appendix C.

5.5 Realistic scenario with MS in the corner

The results obtained so far show that the exploitation of memory can deeply positively affect the performances in cell search procedure. However, in order to improve the advantages that can be obtained by the exploitation of such technique, a different scenario can be devised, in order to emphasize the features that can lead to a more efficient use of the information stored in memory. Moreover, as 5G networks will be characterized by the introduction of new places where mm-wave BSs may be placed, such as lampposts and sides of buildings, such kind of analysis can help to obtain a detailed description of the performances in these environments, in addition to being useful also for current solutions such as WiFi APs. The MSs should be placed in such a way that the BS cannot find them so easily, in order to better emphasize the positive effects of memory. Moreover, the average amount of switches should be higher with respect to the previous scenarios, in order to better exploit the decrease due to memory.

In order to get a more reliable comparison, the scenario must be characterized by similar features with respect to the previous ones. We consider the playground of Chapter 5.4 and keep the same propagation mechanisms, with the only difference that the BS is no more in the center of the deployment area, but it is on the top left corner, while all the other features all the same. An example of such pattern is shown in Figure 5.13.

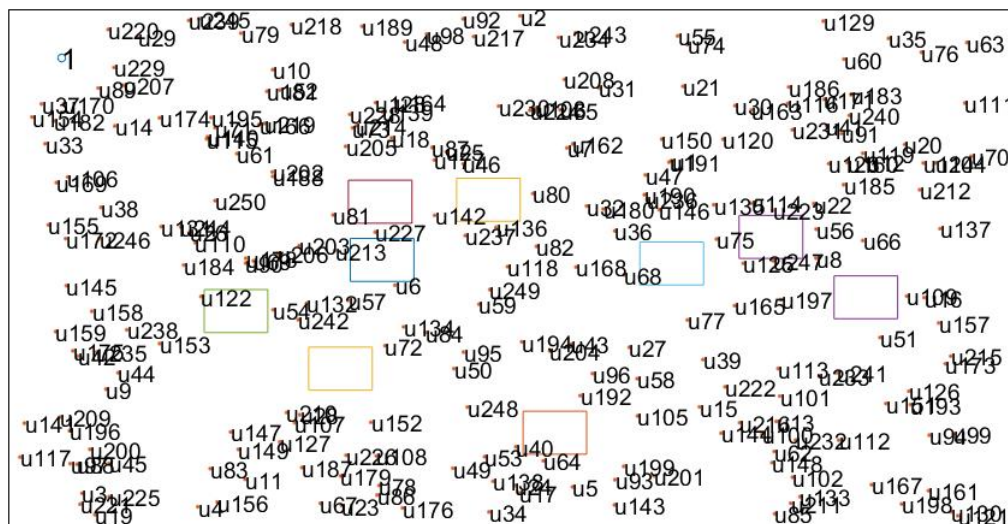


Figure 5.13: New playground representation

The propagation mechanisms are heavily affected by the new environment. When the BS is in the middle of the area, the whole set of configurations can be used to establish LOS transmissions, while, in the new arrangement, a large fraction of the configurations hit almost immediately the walls, and this implies the drawbacks related to reflected beams described in Chapter 5.3. Moreover, the number of unreachable MSs dramatically increases, due to the higher distances from the BS and the greater impact of obstacles, that now shadow a larger percentage area of the

propagation sector. The shift of the BS causes an increase of such amount from an average value of 39.41 to 88.62 MSs.

The comparison with the previous scenario highlights how, in a memoryless environment, performances are definitely worse, as shown in Table 5.17:

Algorithm \ Accuracy [m]	DGS	DGS with centered BS	EDP	EDP with centered BS	Random	Random with centered BS
20	129.66	89.41	77.75	54.44	197.34	130
30	135.29	92.74	80.28	59.33	197.34	130
50	147.21	97.67	86.19	70.12	197.34	130
100	165.57	104.06	100.63	99.83	197.34	130

Table 5.17: Average number of switches with memoryless transmissions

The reason of such worse results is the more deprived location of the BS, that limits the possibility to exploit LOS transmissions and leads to a more widespread exploitation of reflected beams. Despite the higher amount of switches needed in this scenario for all the location error values considered, EDP shows an interesting behavior, as, with the highest location error value, its performance is similar to the outcome of EDP in the previous scenario. An imperfect sector division of the plane heavily affects the cell discovery procedure, however the average distance to the MS is greater, due to the less centralized location of the BS, therefore the effect of the imperfect location mechanism is lower. Moreover, the proximity of the wall can help in diminishing the effects of the reflection, as it introduces only a slight difference in path covered with respect to a direct beam.

The positive influence of memory can be shown in Tables 5.18, 5.19 and 5.20:

Memory range [m] \ Accuracy [m]	5	10	20	30	50	100
20	0.70%	3.30%	7.62%	9.66%	10.82%	11.19%
30	0.62%	2.71%	6.57%	8.96%	10.29%	10.57%
50	0.41%	1.28%	4.01%	5.98%	7.15%	7.36%
100	0.08%	0.50%	1.35%	2.47%	3.18%	3.33%

Table 5.18: Percentage decrease given by memory in DGS algorithm

Memory range [m] \ Accuracy [m]	5	10	20	30	50	100
20	1.36%	4.49%	11.07%	13.92%	14.66%	14.86%
30	0.65%	2.94%	8.02%	11.24%	12.46%	12.61%
50	0.56%	1.74%	4.89%	7.34%	8.85%	9.17%
100	0.08%	0.38%	2.11%	3.45%	4.42%	4.79%

Table 5.19: Percentage decrease given by memory in EDP algorithm

Memory range [m] \ Accuracy [m]	5	10	20	30	50	100
20	1.15%	4.29%	9.61%	11.82%	12.90%	13.24%
30	0.84%	3.09%	7.36%	9.95%	11.39%	11.71%
50	0.43%	1.77%	4.89%	7.15%	8.48%	8.87%
100	0.11%	0.50%	1.88%	3.14%	4.05%	4.41%

Table 5.20: Percentage decrease given by memory in random algorithm

The comparison with the corresponding values in the previous scenario, which can be seen in Tables 5.9, 5.10 and 5.11, shows that the majority of the accuracy-range pairs are characterized by a greater percentage improvement when DGS and EDP are applied, while with random algorithm this behavior can be observed only when more extended memory ranges are considered. However, the reason of such outcome is the higher starting value in terms of number of switches, which can be seen by analyzing the percentage of successful memory accesses with respect to the whole set of accesses, as shown in the next Tables:

Memory range [m] \ Accuracy [m]	5	10	20	30	50	100
20	35.72%	36.56%	30.75%	25.69%	20.70%	17.31%
30	28.75%	28.43%	24.89%	21.91%	18.00%	15.18%
50	18.90%	18.37%	17.00%	15.70%	13.30%	11.50%
100	7.55%	7.85%	8.13%	7.94%	7.30%	6.56%

Table 5.21: Percentage of successful memory accesses with DGS algorithm

Memory range [m] \ Accuracy [m]	5	10	20	30	50	100
20	38.32%	37.91%	31.84%	26.68%	21.50%	17.73%
30	30.93%	29.34%	25.89%	22.72%	18.71%	15.55%
50	19.40%	19.24%	18.12%	16.75%	14.12%	12.02%
100	7.29%	7.72%	8.33%	8.03%	7.32%	6.57%

Table 5.22: Percentage of successful memory accesses with EDP algorithm

Memory range [m] \ Accuracy [m]	5	10	20	30	50	100
20	26.03%	25.72%	21.66%	18.10%	14.75%	12.44%
30	18.51%	19.58%	16.91%	15.17%	12.71%	10.85%
50	12.70%	12.32%	11.29%	10.74%	9.39%	8.23%
100	4.67%	4.70%	5.27%	5.42%	5.10%	4.75%

Table 5.23: Percentage of successful memory accesses with random algorithm

A comparison with the corresponding values stored in Tables 5.12, 5.13 and 5.14 reveals that this scenario is characterized by a more inefficient use of memory, mostly due to the greater impact of obstacles.

CONCLUSIONS AND FUTURE DEVELOPMENTS

This last chapter is dedicated to the conclusions of this thesis work. Chapter 6.1 considers the final outcomes that can be obtained from the simulations analyzed in Chapter 5, while Chapter 6.2 contains some suggestions to future works that can provide better results.

6.1 Conclusions

This thesis work dealt with the comparison of the performances of three algorithms that define an antenna configuration sequence in order to establish a BS-MS connection during cell discovery procedure in a propagation environment exploiting mm-waves. Beamforming techniques were applied to overcome the mm-waves drawbacks related to the shorter wavelength, which increases the path loss and limits the coverage. A localization service allowed the BS to obtain information about the MSs location and consequently properly beamformed. An advanced architecture based on U/C-plane splitting enabled MSs to send such information to the BS through legacy network communications. The comparison of the algorithms was based on the evaluation of their behavior in different localization accuracy levels and environment features. The concept of learning memory technique was applied, enabling the BS to exploit the preceding connections and take advantage of the configurations previously used.

The outcomes of the simulations showed that the possibility to exploit information obtained from the localization service can help in decreasing the average number of switches for a BS-MS connection. The comparison between EDP and DGS, which are based on the MS estimated position, and random algorithm, which neglects such information, emphasized how accurate information about the MS location positively affect the final outcomes. Moreover, the results highlighted how mm-wave technology can be successfully used in the access network and how the exploitation of sophisticated algorithms allows performing cell discovery procedure using a

reasonable amount of switches, with a remarkable improvement with respect to the algorithms that do not exploit context-based information. The accuracy of such information affected to a greater extent the performances of EDP algorithm, as the advantage coming from the sector division of the environment is very dependent on the actual distance between the MS real location and the estimated position. Conversely, DGS was more influenced by the possible presence of obstacles, as they would increase the necessity to exploit reflected beams.

A general behavior of both algorithms was the increase of the average number of switches when the environment conditions, due to the potential presence of obstacles and an uncertainty about the MSs location, reduced the possibility to establish immediately a BS-MS connection exploiting the knowledge of the channel properties. The analysis on a real scenario, characterized by the deployment of obstacles and the uncertainty about the MS location, showed that the application of EDP allows on average to establish a BS-MS connection with a considerably lower number of switches, due to the possibility to focus the transmission in a more restricted area. Despite its simplicity, the use of random algorithm was deprecated as it was characterized by very worse performances.

Moreover, the use of the learning memory procedure could further decrease the average number of switches, due to the possibility to exploit the information about the previous connections. EDP and DGS were characterized by very similar performances in terms of percentage of successful accesses, while random algorithm suffered from the randomness that produced its configuration sequence and therefore its outcome was analogously worse. Furthermore, the optimum memory range size became more extended when worse environment features, in terms of inaccuracy of the MS location information and obstacle deployment, are considered, due to the remarkable improvement coming from a successful memory access and the more cramped impact of an unsuccessful access on final results.

6.2 Future developments

On top of the advantages shown in this work that prove how the application of the learning memory can help in reducing the time spent during the cell search procedure, other techniques can be applied in order to further decrease the average number of switches and consequently obtain better performances. In addition to physical changes of the network, based for example on the deployment of more BSs in the propagation area, refinements in the way used to define the configuration sequence can satisfy this need.

The evaluation of the starting configuration is performed by the BS assuming an obstacle-free scenario. However, a large fraction of the wasted configurations is composed of the ones that hit an obstacle, therefore the BS could save it by evaluating the location of obstacles. A technique that can be used to achieve this goal is based on the previously tested configurations that resulted in an unsuccessful transmission. The BS can suppose that, if a configuration does not reach a

MS, the reason is an impact with an obstacle, therefore it infers that those configurations will hit an obstacle also when they are applied to reach future MSs. This technique can be applied both during the selection of the starting configuration and during the application of the configuration sequence suggested by the algorithm. If the BS assumes that a configuration will hit an obstacle, then it can neglect it from the sequence and skip to the following one. When a sufficient amount of BS-MS connections has been established and consequently a good level of information about the environment can be exploited, the BS can reasonably start to evaluate the obstacle location with positive outcomes. However both the uncertainty about the MSs location and the real obstacle position must be taken into account, therefore the BS cannot be sure about the correctness of its assumptions. The BS can therefore decide to rely on the obstacles information without having full confidence in them and use anyway a configuration even if, according to the collected environment information, that beam would hit an obstacle.

Moreover, when the information stored in memory can be applied, the search procedure begins always with the same configuration used for the nearest MS. However, especially in a scenario with location errors, it may be useful also to exploit the information related to the other MSs that fit in the range of the new MS. A reasonable technique is therefore to start the procedure by analyzing the configurations of more than a single MS. This increase of memory exploitation may result in a greater delay, however an advantage can be obtained by a greater amount of successful memory accesses. A more conservative approach may be chosen, for which only a subset of all the suitable MSs will be employed in order to define the starting set of configurations.



APPENDIX A

The following results are referred to the scenario of Chapter 5.2, in which simulations are performed in an obstacle-free environment with different location error values.

Accuracy [m] / memory range [m]	0	5	10	20	30	50	100
5	6.2362	6.1706	5.9964	5.9476	6.0245	6.1325	6.1911
10	11.2347	11.0782	10.672	10.1714	10.1141	10.1804	10.2359
20	18.7326	18.5083	17.9209	16.8463	16.4855	16.4608	16.5075
30	23.9428	23.7428	23.1818	21.9281	21.3884	21.2870	21.3285
50	29.9078	29.7706	29.3896	28.2689	27.7243	27.4744	27.4943
100	38.7637	38.6754	38.44	38.1046	37.7291	37.5531	37.5254

Table A.1: DGS switches with memory

Accuracy [m] / memory range [m]	0	5	10	20	30	50	100
5	5.3747	5.3613	5.3376	5.3607	5.4527	5.5218	5.5936
10	9.3432	9.2668	9.1647	9.0709	9.0938	9.1106	9.1724
20	16.2992	16.1465	15.9706	15.5978	15.563	15.6379	15.6897
30	23.1064	22.9775	22.7319	22.252	22.1247	22.1068	22.1072
50	36.7447	36.5522	36.1742	35.6292	35.2818	34.9952	34.9726
100	72.2698	72.0405	71.7333	71.2694	70.7615	70.3892	70.3081

Table A.2: EDP switches with memory

Accuracy [m] / memory range [m]	5	10	20	30	50	100
5	12.65	39.41	81.15	96.32	102.15	102.66
10	11.89	37.1	79.24	94.55	99.96	100.45
20	9.71	31.39	70.97	86.69	92	92.52
30	7.58	25.34	60.77	76.18	81.61	82.29
50	4.72	17.17	43.41	57.08	62.88	63.67
100	2.36	7.99	20.67	27.97	32.34	33.41

Table A.3: Successful memory attempts with DGS algorithm

Accuracy [m] / memory range [m]	5	10	20	30	50	100
5	2.01	12.71	56.99	93.86	124.19	140.42
10	2.79	14.48	58.97	96.09	126.36	142.57
20	5.44	21.09	67.26	103.5	134.22	150.54
30	7.36	25.87	76.56	114.34	144.5	160.66
50	9.81	34.81	94.65	132.91	163.36	179.34
100	12.12	42.17	116.01	162.1	194.4	209.96

Table A.4: Unsuccessful memory attempts with DGS algorithm

Accuracy [m] / memory range [m]	5	10	20	30	50	100
5	12.66	39.43	81.19	96.4	102.26	102.76
10	11.84	37.05	79.36	94.79	100.26	100.75
20	9.6	31.29	70.78	86.48	91.82	92.35
30	7.56	25.37	60.88	76.62	82.05	82.77
50	4.7	17.46	43.37	57.02	62.88	63.71
100	2.31	7.98	20.73	27.95	32.19	33.23

Table A.5: Successful memory attempts with EDP algorithm

Accuracy [m] / memory range [m]	5	10	20	30	50	100
5	2	12.69	56.95	93.78	124.08	140.32
10	2.84	14.53	58.85	95.85	126.06	142.27
20	5.55	21.19	67.45	103.71	134.4	150.71
30	7.38	25.84	76.45	113.9	144.06	160.18
50	9.83	34.52	94.69	132.97	163.36	179.3
100	12.17	42.18	115.95	162.12	194.55	210.14

Table A.6: Unsuccessful memory attempts with EDP algorithm

APPENDIX B

The following results are referred to the scenario of Chapter 5.3, in which simulations are performed in an location error-free environment with the deployment of a variable number of obstacles.

obstacles / memory range [m]	0	5	10	20	30	50	100
3	32.1489	31.5648	31.0272	30.5798	30.6216	30.6429	30.6733
6	56.4257	55.3900	54.3431	53.2123	52.9539	52.9326	52.9642
9	77.0317	75.7675	74.0667	72.4668	71.8739	71.8055	71.8018

Table B.1: DGS switches with memory

obstacles / memory range [m]	0	5	10	20	30	50	100
3	16.7991	16.5270	16.2760	16.1127	16.2344	16.3245	16.3783
6	29.2905	28.7042	28.1450	27.5985	27.5335	27.5599	27.6157
9	43.0098	42.2733	41.2999	40.3664	40.1555	40.1671	40.1659

Table B.2: EDP switches with memory

obstacles / memory range [m]	5	10	20	30	50	10
3	12.33	36.78	74.6	88.55	93.81	94.56
6	11.38	33.92	69.45	81.92	86.99	87.93
9	10.6	30.74	62.59	75.07	80.09	80.6

Table B.3: Successful memory attempts with DGS algorithm

obstacles / memory range [m]	5	10	20	30	50	100
3	2.31	14.25	59.48	97.63	131.12	148.17
6	2.6	15.2	60.91	99.38	133.93	153.79
9	2.76	15.21	59.88	97.05	135.28	159.22

Table B.4: Unsuccessful memory attempts with DGS algorithm

obstacles / memory range [m]	5	10	20	30	50	100
3	12.33	36.74	74.51	88.45	93.68	94.43
6	11.38	33.93	69.37	81.88	86.96	87.87
9	10.54	30.63	62.44	74.87	79.89	80.4

Table B.5: Successful memory attempts with EDP algorithm

obstacles / memory range [m]	5	10	20	30	50	100
3	2.31	14.29	59.57	97.72	131.26	148.3
6	2.6	15.19	60.99	99.43	133.96	153.85
9	2.82	15.32	60.03	97.25	135.46	159.42

Table B.6: Unsuccessful memory attempts with EDP algorithm



APPENDIX C

The following results are referred to the scenario of Chapter 5.4, in which simulations are performed in an environment characterized by a variable number of obstacles and different location error values.

Accuracy [m] / memory range [m]	5	10	20	30	50	100	cell size
20	7.23	24.58	55.27	67.68	72.07	72.8	72.83
30	5.54	19.85	47.75	60.12	64.55	65.34	65.37
50	3.92	13.92	35.26	46.24	51.55	52.12	52.17
100	1.92	6.42	17.57	23.63	27.62	28.67	28.69

Table C.1: Successful memory attempts with DGS algorithm

Accuracy [m] / memory range [m]	5	10	20	30	50	100	cell size
20	5.59	21.89	68.15	105.71	144.06	167.5	176.03
30	7.17	26.07	74.99	113.68	152.17	175.37	183.49
50	9.22	30.88	87.97	128.98	166.13	188.91	196.69
100	11.12	38.13	106.88	153.41	191.87	212.75	220.17

Table C.2: Unsuccessful memory attempts with DGS algorithm

Accuracy [m] / memory range [m]	5	10	20	30	50	100	cell size
20	7.16	24.52	55.12	67.59	72.04	72.83	72.86
30	5.47	19.73	47.6	59.84	64.34	65.07	65.11
50	3.95	13.82	35.14	45.99	51.31	51.88	51.93
100	1.89	6.5	17.26	23.13	27.27	28.13	28.17

Table C.3: Successful memory attempts with EDP algorithm

Accuracy [m] / memory range [m]	5	10	20	30	50	100	cell size
20	5.66	21.95	68.3	105.8	144.09	167.47	176
30	7.24	26.19	75.15	113.97	152.38	175.64	183.75
50	9.19	30.98	88.09	129.23	166.37	189.15	196.93
100	11.15	38.05	107.18	153.9	192.22	213.29	220.69

Table C.4: Unsuccessful memory attempts with EDP algorithm

Accuracy [m] / memory range [m]	5	10	20	30	50	100	cell size
20	4.08	14.74	33.89	41.69	44.64	45.57	45.63
30	3.08	11.13	28.1	35.91	39.09	39.95	40.01
50	2.18	7.04	18.65	25.42	28.92	29.79	29.86
100	1.09	3.52	9.52	13.17	15.61	16.43	16.47

Table C.5: Successful memory attempts with random algorithm

Accuracy [m] / memory range [m]	5	10	20	30	50	100	cell size
20	8.74	31.73	89.53	131.7	171.49	194.73	203.23
30	9.63	34.79	94.64	137.89	177.63	200.76	208.85
50	10.96	37.76	104.58	149.8	188.76	211.24	219
100	11.95	41.03	114.93	163.87	203.88	224.99	232.39

Table C.6: Unsuccessful memory attempts with random algorithm

Accuracy [m] / memory range [m]	5	10	20	30	50	100	cell size
20	11.7371	11.8515	10.4035	8.6426	7.2793	6.543	6.2916
30	9.0927	8.8051	8.668	7.7793	6.7492	6.1077	5.8814
50	6.9729	6.4349	5.6974	5.7816	5.3687	4.876	4.6963
100	3.8081	3.0474	3.0211	2.8193	2.8992	2.7039	2.5961

Table C.7: Average amount of saved switches for every memory access with DGS algorithm

Accuracy [m] / memory range [m]	5	10	20	30	50	100	cell size
20	20.8119	22.4060	23.2314	22.1415	21.8297	21.5973	21.4984
30	20.8607	20.3692	22.2810	22.4891	22.6598	22.5004	22.3902
50	23.3734	20.7102	19.9117	21.9084	22.6704	22.5493	22.4023
100	25.8636	21.1466	21.3989	21.1229	23.0396	22.7685	22.5184

Table C.8: Average amount of saved switches for every successful memory access with DGS algorithm

Accuracy [m] / memory range [m]	5	10	20	30	50	100	cell size
20	150.47	550.74	1284.00	1498.54	1573.27	1572.29	1565.73
30	115.57	404.33	1063.92	1352.05	1462.69	1470.18	1463.65
50	91.62	288.29	702.09	1013.05	1168.66	1175.27	1168.73
100	49.66	135.76	375.98	499.13	636.36	652.77	646.05

Table C.9: Average amount of saved switches in each pattern with DGS algorithm

Accuracy [m] / memory range [m]	5	10	20	30	50	100	cell size
20	5.9116	5.7985	5.3783	4.1149	3.6221	3.3090	3.1690
30	5.2062	5.0267	4.6598	4.2284	3.4373	3.1140	2.9861
50	4.1071	3.8569	3.5327	3.2144	2.7763	2.5656	2.4306
100	3.3930	2.4931	2.6141	2.5981	2.7748	2.5572	2.4437

Table C.10: Average amount of saved switches for every memory access with EDP algorithm

Accuracy [m] / memory range [m]	5	10	20	30	50	100	cell size
20	10.5848	10.9893	12.0426	10.5559	10.8669	10.9180	10.8241
30	12.0971	11.6993	12.0166	12.2817	11.5780	11.5195	11.4132
50	13.6626	12.5028	12.3886	12.2467	11.7782	11.9195	11.6481
100	23.4099	17.0875	18.8471	19.8853	22.3337	21.9467	21.5881

Table C.11: Average amount of saved switches for every successful memory access with EDP algorithm

Accuracy [m] / memory range [m]	5	10	20	30	50	100	cell size
20	75.79	269.47	663.79	788.48	782.85	795.16	788.64
30	66.27	230.83	571.99	734.94	744.93	749.57	743.11
50	54.06	172.88	435.34	563.23	604.34	618.38	604.88
100	44.24	111.07	325.29	459.95	609.04	617.36	608.14

Table C.12: Average amount of saved switches in each pattern with EDP algorithm

Accuracy [m] / memory range [m]	5	10	20	30	50	100	cell size
20	29.88	31.94	27.00	22.70	19.26	17.67	17.05
30	23.92	22.83	21.52	19.04	16.61	15.33	14.81
50	15.26	14.60	12.79	12.50	11.72	10.93	10.57
100	6.26	5.78	5.96	5.85	5.64	5.42	5.24

Table C.13: Average amount of saved switches for each memory access with random algorithm

Accuracy [m] / memory range [m]	5	10	20	30	50	100	cell size
20	93.8889	100.6887	98.3386	94.4069	93.2685	93.1709	92.9831
30	98.7216	94.2065	94.0063	92.1348	92.0777	92.3607	92.1353
50	91.9653	92.8938	84.5072	86.1522	88.2368	88.4569	88.1303
100	74.9315	73.1205	77.8650	78.6659	79.2616	79.6158	79.1932

Table C.14: Average amount of saved switches for every successful memory access with random algorithm

Accuracy [m] / memory range [m]	5	10	20	30	50	100	cell size
20	383.07	1484.15	3332.70	3935.82	4163.50	4245.80	4242.82
30	304.06	1048.52	2641.58	3308.56	3599.32	3689.81	3686.33
50	200.48	653.97	1576.06	2189.99	2551.81	2635.13	2631.57
100	81.68	257.38	741.27	1036.03	1237.27	1308.09	1304.31

Table C.15: Average amount of saved switches in each pattern with random algorithm

BIBLIOGRAPHY

- [1] NGMN Alliance, “NGMN 5G White Paper.” Available at https://www.ngmn.org/uploads/media/NGMN_5G_White_Paper_V1_0.pdf (2016/02/28), February 2015.
- [2] Ericsson, “Ericsson mobility report.” Available at <http://www.ericsson.com/res/docs/2015/mobility-report/ericsson-mobility-report-nov-2015.pdf> (2016/02/28), November 2015.
- [3] D. Evans, “The internet of things - how the next evolution of the internet is changing everything.” Available at http://www.cisco.com/c/dam/en_us/about/ac79/docs/innov/IoT_IBSG_0411FINAL.pdf (2016/02/28), Apr 2011.
- [4] Huawei, “5g: A technology vision.” Available at <http://www.huawei.com/5gwhitepaper/> (2016/02/28), 2013.
- [5] R. Ratasuk, D. Tolli, and A. Ghosh, “Carrier aggregation in lte-advanced,” in *Vehicular Technology Conference (VTC 2010-Spring)*, 2010 IEEE 71st, pp. 1–5, May 2010.
- [6] Ericsson, “5g radio access.” Available at <http://www.ericsson.com/res/docs/whitepapers/wp-5g.pdf> (2016/02/28), 02 2015.
- [7] Samsung Electronics, “5g vision.” Available at <http://www.samsung.com/global/business-images/insights/2015/Samsung-5G-Vision-0.pdf> (2016/02/28), 02 2015.
- [8] Ericsson, “Iot, 5g, big data.” Available at http://eucnc.eu/files/2015/presentations/panel2/01_07_2015_EUCNC_Paris_IoT_5G_SD_Panel_D.Pakiry_ERICSSON_Final.pdf (2016/02/28).
- [9] E. Lähetkangas, K. Pajukoski, J. Vihriälä, G. Berardinelli, M. Lauridsen, E. Tirola, and P. Mogensen, “Achieving low latency and energy consumption by 5g tdd mode optimization,” in *Communications Workshops (ICC), 2014 IEEE International Conference on*, pp. 1–6, June 2014.
- [10] T. Rappaport, J. Murdock, and F. Gutierrez, “State of the art in 60-ghz integrated circuits and systems for wireless communications,” *Proceedings of the IEEE*, vol. 99, pp. 1390–1436, Aug 2011.

- [11] B. Song, *MicroCMOS Design*. Circuits and Electrical Engineering, Taylor & Francis, 2011.
- [12] S. Rangan, T. Rappaport, and E. Erkip, "Millimeter-wave cellular wireless networks: Potentials and challenges," *Proceedings of the IEEE*, vol. 102, pp. 366–385, March 2014.
- [13] GSMA Intelligence, "Understanding 5g: Perspectives on future technological advancements in mobile." Available at <https://gsmaintelligence.com/research/?file=141208-5g.pdf&download> (2016/02/28), December 2014.
- [14] S. Yi, S. Chun, Y. Lee, S. Park, and S. Jung, *Radio Protocols for LTE and LTE-Advanced*. Wiley, 2012.
- [15] Nokia Networks, "5g use cases and requirements." Available at http://networks.nokia.com/sites/default/files/document/5g_requirements_white_paper.pdf (2016/02/28).
- [16] A. Technologies, *LTE and the Evolution to 4G Wireless: Design and Measurement Challenges*. John Wiley & Sons, 2009.
- [17] A. Maltsev, A. Pudeyev, I. Bolotin, G. Morozov, I. Karls, M. Faerber, I. Siaud, A.-M. Ulmer-Moll, J.-M. Conrat, R. Weiler, and M. Peter, "Wp5: Propagation, antennas and multi-antenna techniques - d5.1: Channel modeling and characterization," tech. rep., 06 2014.
- [18] J. Hoadley and P. Maveddat, "Enabling small cell deployment with hetnet," *Wireless Communications, IEEE*, vol. 19, pp. 4–5, April 2012.
- [19] E. Tiedemann, "5g: The next generation (big wave) of wireless." Available at https://www.nttdocomo.co.jp/binary/pdf/corporate/technology/rd/tech/5g/NTTDOCOMO_5G_TBS_lecture6.pdf (2016/02/28).
- [20] K. Sakaguchi, G. K. Tran, H. Shimodaira, S. Nanba, T. Sakurai, K. Takinami, I. Siaud, E. C. Strinati, A. Capone, I. Karls, R. Arefi, and T. Haustein, "Millimeter-wave evolution for 5g cellular networks," *CoRR*, vol. abs/1412.3212, 2014.
- [21] D. Liu, J. Akkermans, H.-C. Chen, and B. Floyd, "Packages with integrated 60-ghz aperture-coupled patch antennas," *Antennas and Propagation, IEEE Transactions on*, vol. 59, pp. 3607–3616, Oct 2011.
- [22] P. Smulders, H. Yang, and I. Akkermans, "On the design of low-cost 60-ghz radios for multigigabit-per-second transmission over short distances [topics in radio communications]," *Communications Magazine, IEEE*, vol. 45, pp. 44–51, December 2007.

- [23] R. Weiler, M. Peter, W. Keusgen, E. Calvanese-Strinati, A. De Domenico, I. Filippini, A. Capone, I. Siaud, A.-M. Ulmer-Moll, A. Maltsev, T. Haustein, and K. Sakaguchi, "Enabling 5g backhaul and access with millimeter-waves," in *Networks and Communications (EuCNC), 2014 European Conference on*, pp. 1–5, June 2014.
- [24] U. Johannsen, M. I. Kazim, A. B. Smolders, and M. H. A. J. Herben, "Modular antenna array concept for millimeter-wave beam-steering applications," in *Progress In Electromagnetics Research Symposium Proceedings*, pp. 229–233, August 2013.
- [25] METIS, "Deliverable D1.5 - Updated scenarios, requirements and KPIs for 5G mobile and wireless system with recommendations for future investigations." Available at https://www.metis2020.com/wp-content/uploads/deliverables/METIS_D1.5_v1.pdf (2016/02/28), 2015.
- [26] H. Tullberg, P. Popovski, D. Gozalvez-Serrano, P. Fertl, Z. Li, A. Höglund, M. A. Uusitalo, H. Droste, O. Bulakci, J. Eichinger, and K. Pawlak, "METIS System Concept: The Shape of 5G to Come." Available at https://www.metis2020.com/wp-content/uploads/publications/IEEE_CommMag_2015_Tullberg_etal_METIS-System-Concept.pdf (2016/02/28), 2015.
- [27] E. G. Ström, P. Popovski, and J. Sachs, "5g ultra-reliable vehicular communication," *CoRR*, vol. abs/1510.01288, 2015.
- [28] H. Zhao, R. Mayzus, S. Sun, M. Samimi, J. Schulz, Y. Azar, K. Wang, G. Wong, F. Gutierrez, and T. Rappaport, "28 ghz millimeter wave cellular communication measurements for reflection and penetration loss in and around buildings in new york city," in *Communications (ICC), 2013 IEEE International Conference on*, pp. 5163–5167, June 2013.
- [29] S. Nie, G. Maccartney, S. Sun, and T. Rappaport, "28 ghz and 73 ghz signal outage study for millimeter wave cellular and backhaul communications," in *Communications (ICC), 2014 IEEE International Conference on*, pp. 4856–4861, June 2014.
- [30] J. J. Hamad-Ameen, "Cell planning in gsm mobile," *WTOC*, vol. 7, pp. 393–398, May 2008.
- [31] A. Daeinabi, K. Sandrasegaran, and X. Zhu, "Survey of intercell interference mitigation techniques in lte downlink networks," in *Telecommunication Networks and Applications Conference (ATNAC), 2012 Australasian*, pp. 1–6, Nov 2012.
- [32] H. Song, X. Fang, and L. Yan, "Handover scheme for 5g c/u plane split heterogeneous network in high-speed railway," *Vehicular Technology, IEEE Transactions on*, vol. 63, pp. 4633–4646, Nov 2014.
- [33] J. Rodriguez, *Fundamentals of 5G Mobile Networks*. Wiley, 2015.

- [34] B. Singh, S. Hailu, K. Koufos, A. Dowhuszko, O. Tirkkonen, R. Jäntti, and R. Berry, “Coordination protocol for inter-operator spectrum sharing in co-primary 5g small cell networks,” *Communications Magazine, IEEE*, vol. 53, pp. 34–40, July 2015.
- [35] Mobile and wireless communications Enablers for the Twenty-twenty Information Society (METIS), “Deliverable d5.1 - intermediate description of the spectrum needs and usage principles.” Available at https://www.metis2020.com/wp-content/uploads/deliverables/METIS_D5.1_v1.pdf (2016/02/28).
- [36] C. Anderson, T. Rappaport, K. Bae, A. Verstak, N. Ramakrishnan, W. Tranter, C. Shaffer, and L. Watson, “In-building wideband multipath characteristics at 2.5 and 60 ghz,” in *Vehicular Technology Conference, 2002. Proceedings. VTC 2002-Fall. 2002 IEEE 56th*, vol. 1, pp. 97–101 vol.1, 2002.
- [37] A. Falaschi, *Elementi di trasmissione dei segnali e sistemi di telecomunicazione*. Aracne, 2009.
- [38] P. Karadimas, B. Allen, and P. Smith, “Human body shadowing characterization for 60-ghz indoor short-range wireless links,” *Antennas and Wireless Propagation Letters, IEEE*, vol. 12, pp. 1650–1653, 2013.
- [39] M. Peter, M. Wisotzki, M. Raceala-Motoc, W. Keusgen, R. Felbecker, M. Jacob, S. Priebe, and T. Kurner, “Analyzing human body shadowing at 60 ghz: Systematic wideband mimo measurements and modeling approaches,” in *Antennas and Propagation (EUCAP), 2012 6th European Conference on*, pp. 468–472, March 2012.
- [40] R. C. Daniels and R. W. H. Jr., “60 ghz wireless communications: emerging requirements and design recommendations,” *IEEE Vehicular Technology Magazine*, vol. 2, pp. 41–50, Sept 2007.
- [41] B. Langen, G. Lober, and W. Herzig, “Reflection and transmission behaviour of building materials at 60 ghz,” in *Personal, Indoor and Mobile Radio Communications, 1994. Wireless Networks - Catching the Mobile Future., 5th IEEE International Symposium on*, pp. 505–509 vol.2, Sep 1994.
- [42] M. Ergen, *Mobile Broadband: Including WiMAX and LTE*. Information Technology: Transmission, Processing and Storage, Springer US, 2009.
- [43] A. Maltsev, E. Perahia, R. Maslennikov, A. Sevastyanov, A. Lomayev, and A. Khoryaev, “Impact of polarization characteristics on 60-ghz indoor radio communication systems,” *Antennas and Wireless Propagation Letters, IEEE*, vol. 9, pp. 413–416, 2010.
- [44] F. Yildirim, A. Sadri, and H. Liu, “Polarization effects for indoor wireless communications at 60 ghz,” *Communications Letters, IEEE*, vol. 12, pp. 660–662, September 2008.

- [45] A. Lebedev, X. Pang, J. Vegas Olmos, S. Forchhammer, I. Tafur Monroy, M. Beltran, and R. Llorente, "Fiber-supported 60 ghz mobile backhaul links for access/metropolitan deployment," in *Optical Network Design and Modeling (ONDM), 2013 17th International Conference on*, pp. 190–193, April 2013.
- [46] "Iso/iec/ieee international standard for information technology–telecommunications and information exchange between systems–local and metropolitan area networks–specific requirements–part 11: Wireless lan medium access control (mac) and physical layer (phy) specifications amendment 3: Enhancements for very high throughput in the 60 ghz band (adoption of ieee std 802.11ad-2012)," *ISO/IEC/IEEE 8802-11:2012/Amd.3:2014(E)*, pp. 1–634, March 2014.
- [47] A. Goldsmith, *Wireless Communications*. Cambridge University Press, 2005.
- [48] M. Ghavami, L. Michael, and R. Kohno, *Ultra Wideband Signals and Systems in Communication Engineering*. Wiley, 2004.
- [49] E. Dahlman, S. Parkvall, and J. Skold, *4G: LTE/LTE-Advanced for Mobile Broadband: LTE/LTE-Advanced for Mobile Broadband*. Elsevier Science, 2011.
- [50] G. de Alwis, M. Delahoy, S. Planning, E. Team, R. P. Group, and A. C. Authority, "60 ghz band millimetre wave technology." Available at http://www.acma.gov.au/webwr/radcomm/frequency_planning/radiofrequency_planning_topics/docs/sp3_04_60%20ghz%20mwt%20-%20discussion%20paper-final.pdf (2016/02/28), 2004.
- [51] Y. Niu, Y. Li, D. Jin, L. Su, and A. V. Vasilakos, "A survey of millimeter wave (mmwave) communications for 5g: Opportunities and challenges," *CoRR*, vol. abs/1502.07228, 2015.
- [52] S. L. Cotton and W. G. Scanlon, "Millimeter-wave soldier-to-soldier communications for covert battlefield operations," 2009.
- [53] K. Murphy, R. Appleby, G. Sinclair, A. McClumpha, K. Tatlock, R. Doney, and I. Hutcheson, "Millimetre wave aviation security scanner," in *Security Technology, 2002. Proceedings. 36th Annual 2002 International Carnahan Conference on*, pp. 162–166, 2002.
- [54] H. S. Ghadikolaei, C. Fischione, P. Popovski, and M. Zorzi, "Design aspects of short range millimeter wave networks: A MAC layer perspective," *CoRR*, vol. abs/1509.07538, 2015.
- [55] A. Maltsev, A. Pudueyev, I. Karls, I. Bolotin, G. Morozov, R. Weiler, M. Peter, and W. Keusgen, "Quasi-deterministic approach to mmwave channel modeling in a non-stationary environment," in *Globecom Workshops (GC Wkshps), 2014*, pp. 966–971, Dec 2014.

- [56] M. Park and P. Gopalakrishnan, "Analysis on spatial reuse and interference in 60-ghz wireless networks," *Selected Areas in Communications, IEEE Journal on*, vol. 27, pp. 1443–1452, October 2009.
- [57] E. Mohamed, K. Sakaguchi, and S. Sampei, "Millimeter wave beamforming based on wifi fingerprinting in indoor environment," in *Communication Workshop (ICCW), 2015 IEEE International Conference on*, pp. 1155–1160, June 2015.
- [58] H. Ishii, Y. Kishiyama, and H. Takahashi, "A novel architecture for lte-b :c-plane/u-plane split and phantom cell concept," in *Globecom Workshops (GC Wkshps), 2012 IEEE*, pp. 624–630, Dec 2012.
- [59] L. Yan and X. Fang, "Reliability evaluation of 5g c/u-plane decoupled architecture for high-speed railway," *EURASIP Journal on Wireless Communications and Networking*, vol. 2014, no. 1, pp. 1–11, 2014.
- [60] L. Yang and W. Zhang, *Interference Coordination for 5G Cellular Networks*. SpringerBriefs in Electrical and Computer Engineering, Springer International Publishing, 2015.
- [61] R. Wang, H. Hu, and X. Yang, "Potentials and challenges of c-ran supporting multi-rats toward 5g mobile networks," *Access, IEEE*, vol. 2, pp. 1187–1195, 2014.
- [62] P. Chanclou, A. Pizzinat, F. Le Clech, T.-L. Reedeker, Y. Lagadec, F. Saliou, B. Le Guyader, L. Guillo, Q. Deniel, S. Gosselin, S. Le, T. Diallo, R. Brenot, F. Lelarge, L. Marazzi, P. Parolari, M. Martinelli, S. O'Dull, S. Gebrewold, D. Hillerkuss, J. Leuthold, G. Gavioli, and P. Galli, "Optical fiber solution for mobile fronthaul to achieve cloud radio access network," in *Future Network and Mobile Summit (FutureNetworkSummit), 2013*, pp. 1–11, July 2013.
- [63] M. Maier and N. Ghazisaidi, *FiWi Access Networks*. New York, NY, USA: Cambridge University Press, 1st ed., 2012.
- [64] D. Nasset, "Ng-pon2 technology and standards," *Lightwave Technology, Journal of*, vol. 33, pp. 1136–1143, March 2015.
- [65] China Mobile Research Institute, "C-ran the road towards green ran." Available at http://labs.chinamobile.com/cran/wp-content/uploads/CRAN_white_paper_v2_5_EN.pdf (2016/02/28).
- [66] J. Wu, Z. Zhang, Y. Hong, and Y. Wen, "Cloud radio access network (c-ran): a primer," *Network, IEEE*, vol. 29, pp. 35–41, Jan 2015.

- [67] C. Lanzani, G. Kardaras, and D. Boppana, "Remote radio heads and the evolution towards 4g networks," 2009.
- [68] H.-N. Dai, K.-W. Ng, M. Li, and M.-Y. Wu, "An overview of using directional antennas in wireless networks," 2013.
- [69] Q. Li, H. Niu, G. Wu, and R. Hu, "Anchor-booster based heterogeneous networks with mmwave capable booster cells," in *Globecom Workshops (GC Wkshps), 2013 IEEE*, pp. 93–98, Dec 2013.
- [70] "Lte; evolved universal terrestrial radio access (e-utra) and evolved universal terrestrial radio access network (e-utran); overall description; stage 2." Available at http://www.etsi.org/deliver/etsi_ts/136300_136399/136300/09.04.00_60/ts_136300v090400p.pdf (2016/02/28).
- [71] Y. Kim and K. Chang, "Complexity optimized cp length pre-decision metric for cell searcher in the downlink of 3gpp lte system," in *Personal, Indoor and Mobile Radio Communications, 2009 IEEE 20th International Symposium on*, pp. 895–899, Sept 2009.
- [72] C. Barati, S. Hosseini, S. Rangan, P. Liu, T. Korakis, S. Panwar, and T. Rappaport, "Directional cell discovery in millimeter wave cellular networks," *Wireless Communications, IEEE Transactions on*, vol. 14, pp. 6664–6678, Dec 2015.
- [73] V. L. F. Richard Yu, *Advances in Mobile Cloud Computing Systems*. CRC Press.
- [74] A. Capone, I. Filippini, and V. Sciancalepore, "Context information for fast cell discovery in mm-wave 5g networks," in *European Wireless 2015; 21th European Wireless Conference; Proceedings of*, pp. 1–6, May 2015.
- [75] A. Capone, I. Filippini, V. Sciancalepore, and D. Tremolada, "Obstacle avoidance cell discovery using mm-waves directive antennas in 5g networks," in *Personal, Indoor, and Mobile Radio Communications (PIMRC), 2015 IEEE 26th Annual International Symposium on*, pp. 2349–2353, Aug 2015.
- [76] R. Di Taranto, S. Muppisetty, R. Raulefs, D. Slock, T. Svensson, and H. Wymeersch, "Location-aware communications for 5g networks: How location information can improve scalability, latency, and robustness of 5g," *Signal Processing Magazine, IEEE*, vol. 31, pp. 102–112, Nov 2014.
- [77] C. Kee and B. Parkinson, "Wide area differential gps as a future navigation system in the u.s.," in *Position Location and Navigation Symposium, 1994., IEEE*, pp. 788–795, Apr 1994.

- [78] A. El-Rabbany, *Introduction to GPS: The Global Positioning System*. Artech House mobile communications series, Artech House, 2002.
- [79] C. Feng, W. Au, S. Valaee, and Z. Tan, "Received-signal-strength-based indoor positioning using compressive sensing," *Mobile Computing, IEEE Transactions on*, vol. 11, pp. 1983–1993, Dec 2012.